

AD-A084 623

ARCTEC INC COLUMBIA MD

F/G 13/10

MODEL TESTS IN ICE TO CONFIRM EFFECTIVENESS OF THE 140-FOOT WYT--ETC(U)

AUG 77 R A MAJOR

DOT-C8-6424A

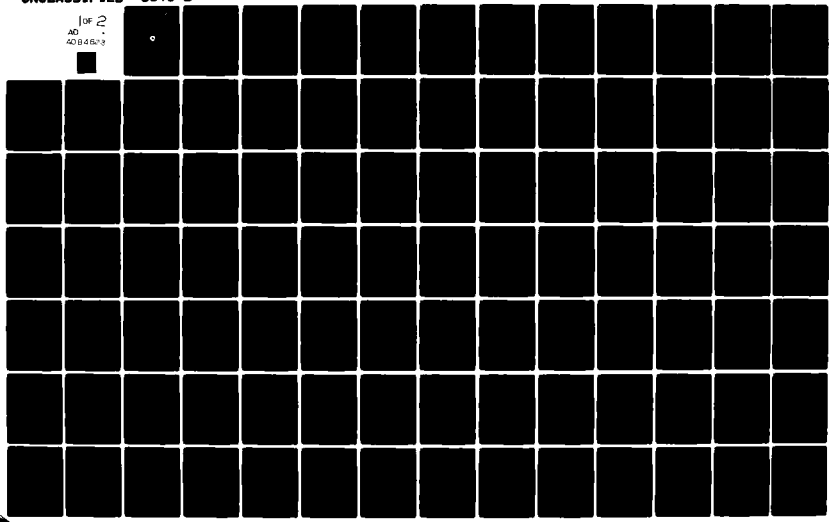
UNCLASSIFIED

354C-2

USCG-E-02-80

NL

1 of 2
AD
408487/2



Report No. CG-E-02-80

LEVEL II

(13)

ADA 084623

MODEL TESTS IN ICE TO CONFIRM
EFFECTIVENESS OF THE 140-FOOT
WTYM AIR BUBBLER SYSTEM



AUGUST 1977

Document is available to the public through the
National Technical Information Service,
Springfield, Virginia 22151

DTIC
ELECTE
MAY 27 1980

Prepared for

**U.S. DEPARTMENT OF TRANSPORTATION
United States Coast Guard**

NAVAL ENGINEERING DIVISION

WASHINGTON, DC 20595
THE COPY FURNISHED TO DDC CONTAINED A
SIGNIFICANT NUMBER OF PAGES WHICH DO NOT
REPRODUCE LEGIBLY.

405-535

80 5 23 056

DISCLAIMER NOTICE

THIS DOCUMENT IS BEST QUALITY PRACTICABLE. THE COPY FURNISHED TO DTIC CONTAINED A SIGNIFICANT NUMBER OF PAGES WHICH DO NOT REPRODUCE LEGIBLY.

NOTICE

This document is disseminated under the sponsorship of the Department of Transportation in the interest of information exchange. The United States Government assumes no liability for its contents or use thereof.

The contents of this report do not necessarily reflect the official view or policy of the Coast Guard; and they do not constitute a standard, specification, or regulation.

This report, or portions thereof may not be used for advertising or sales promotion purposes. Citation of trade names and manufacturers does not constitute endorsement or approval of such products.

Accession For	
NTIS GARDI	<input checked="" type="checkbox"/>
DOC TAB	<input type="checkbox"/>
Unannounced	<input type="checkbox"/>
Justification	
By _____	
Distribution/	
Applicable Codes	
Dist	Number/for special
A	23

1 Report No. CG-E-02-08	2 Government Accession No. AD-A084 623	3 Recipient's Catalog No.
4 Title and Subtitle Model Tests in ice to confirm effectiveness of the 140' WYTM Air Bubbler System		5 Date of Publication 1 August 1977
6 Authoring Robert A. Major	7 Performing Organization Code 354C-2	8 Performing Organization Report No. 12 106
9 Sponsoring Agency Name and Address ARCTEC INC. 9104 Red Branch Road Columbia, MD 21045	10 Work Unit No. (if applicable) 15	11 Contract or Grant No. DOT-CG-6424A
12 Sponsoring Agency Name and Address Commandant (G-ENE) U.S. Coast Guard 2100 2nd St. S.W. Washington, D.C. 20593	13 Type of Report and Period Covered Model Test Report 1977	14 Sponsoring Agency Code G-ENE

15 Supplementary Notes

16 Abstract

A 1/24th scale model of the 150 FT. WYTM was equipped with an air bubbler system. The bubbler system was operated at various flow rates from no flow to twice the nominal system capacity. Tests were performed in both solid ice and brash to determine the effectiveness of the bubbler system in reducing the power required to transit ice fields. In all cases, a flow was found which reduced the total power from that required for a ship without the air system. This model test formed the basis for designing the air bubbler system for the Coast Guard 140' class of icebreaking tugs.

17 Key Words Air Bubbler System Icebreaking Model Tests in Ice	18 Distribution Statement Document is available to the public through the National Technical Information Service, Springfield, VA 22161
--	---

19 Security Classification of this report Unclassified	20 Security Class. (of this page) Unclassified	21 No. of Pages 101	22 Price
--	--	-------------------------------	----------

ARCTEC, Incorporated

REPORT No. 354C-2

MODEL TESTS IN ICE TO CONFIRM
EFFECTIVENESS OF THE 140 FT.
WYTM AIR BUBBLER SYSTEM

by

Robert A. Major

February 28, 1977

Revised

August 1, 1977

Contract DOT-CG-64,242A

For

Commandant (G-ENE-3/64)
U.S. Coast Guard
Washington, D.C. 20590

Submitted by

ARCTEC, Incorporated
9104 Red Branch Road
Columbia, Maryland 21045

ABSTRACT

A 1/24th scale model of the 150 FT. WYTM was equipped with an air bubbler system. The bubbler system was operated at various flow rates from no flow to twice the nominal system capacity. Tests were performed in both solid ice and brash to determine the effectiveness of the bubbler system in reducing the power required to transit ice fields. In all cases, a flow was found which reduced the total power from that required for a ship without the air system.

This document has been approved
for public release and sale; its
distribution is unlimited.

NOMENCLATURE

B	Beam
C_0-C_5	Coefficients of Regression Equations
E	Elastic Modulus of the Ice Sheet
I	Mass Moment of Inertia
L	Length
M	Mass
P	Power
Q	Volume Flow
R	Resistance or gas constant
T	Temperature
W	Work
f	Coefficient of Kinetic Friction (friction factor)
g	Acceleration due to Gravity
h	Ice Thickness
k	Ratio of specific heats for a Gas
λ_c	Characteristic Length of the Ice Sheet
p	Pressure
t	Time, thrust deduction fraction
v	Speed
W_T	Thrust identity wake fraction
λ	Ship-Model Geometric Scale Ratio
ρ_i	Mass Density of Ice
ρ_w	Mass Density of Water
σ_f	Flexural Strength of Ice Sheet

TABLE OF CONTENTS

	Page
ABSTRACT	<i>i</i>
NOMENCLATURE	<i>ii</i>
1. SUMMARY	1-1
2. MODEL AND TEST DESCRIPTION	2-1
3. TEST RESULTS	3-1
4. ANALYSIS	4-1
5. CONCLUSIONS AND RECOMMENDATIONS	5-1
6. REFERENCES	6-1
APPENDICES	
A. RESISTANCE DATA	A-1
B. FRICTION DATA	B-1
C. ICE DATA	C-1
D. REGRESSION ANALYSIS	D-1
E. METHOD OF SCALING BUBBLER SYSTEM CHARACTERISTICS	E-1

1. SUMMARY

The purpose of this series of tests was to determine what airflow to the air bubbler system on the Coast Guard 140-FT WYTM is most effective in increasing icebreaking performance. The bubbler system was modeled for 1.5 ft. of solid ice and 3.0 ft. of brash ice. Three speeds, 1, 3, and 5 knots full-scale, plus static resistance were examined. A range of six flow rates was covered from the least flow required to decrease resistance to the point where increasing flow had little additional effect. The most effective airflow is that representing the lowest total horsepower, adding air compressor power to shaft horsepower at each of the three speeds and in static conditions. The following Table summarizes test results.

BUBBLER FLOW FOR LEAST REQUIRED HORSEPOWER

<u>Ice Type</u>	<u>Thickness</u>	<u>Speed, Kts</u>	<u>Bubbler Flow SCFM</u>	<u>Total Horsepower</u>
Solid Ice	1.7 ft.	0	5,000	1,770**
		1	7,500	2,050
	1.5 ft.	3	6,500	2,900
		5	6,000	3,450
		5	6,000	3,450
Brash Ice	3.5 ft.	0	4,000	600
		1	13,000	1,870
	6.0 ft.***	3	11,500	2,120
		5	8,500	2,250
		5	8,500	2,250

The performance of the 140-FT WYTM in solid ice without an air bubbler system has been determined in earlier tests [1]*. In these earlier tests, the change in resistance with varying hull-ice friction was also examined. In the present tests, a constant hull-ice friction of 0.23 was used.

The 140-FT WYTM bubbler system is designed for an airflow of 7500 SCFM [2]. Manifold cross sections and orifice sizes are based on this flow. Variations in manifold pressure with flow rate are found in the design report [2]. The evaluation above is based on a constant piping system.

In addition to the collection of resistance data, this program also included high-speed underwater movies. These films may be

* References listed in Section 6.

** Weak Ice

*** Extrapolated from test conditions

used to evaluate the placement of nozzles in planning for possible different arrangements on new designs, such as the proposed Great Lakes-Arctic East Icebreaker. They clearly show air flow patterns and may be used also to determine if air will be injected into seachests. The movies indicate that additional nozzles further forward might be helpful. Seachests located near the keel appear unlikely to inject air.

2. MODEL AND TEST DESCRIPTION

2.1 Model

A wooden model, constructed to the molded lines of the 140 FT WYTM, was used in these tests. This same model was used for the tests conducted earlier [1]. Table 2.1 contains the particulars of the full-scale tug and the 1/24th scale model while Figure 2.1 is an abbreviated version of the lines. In addition to the rudder, an appendage representing the bubbler duct below the keel forward was added to the model. This was added to ensure that bubbler flow did not cross the keel since orifice placement is slightly higher than the full-scale nozzles. Figure 2.2 shows the difference between orifice placement on the model and on the full-scale ship for the bow manifolds.

2.2 Bubbler System

Each of the four manifolds on the ship was separately modeled and instrumented. All orifice sizes were 1/16 in. (1.6 mm) which represents 1.5 in. full-scale. Figure 2.3 is a schematic of the model bubbler system. The flowmeters utilized were Brooks Instrument Model 1355 Sho-Rate 150's on each manifold. These were factory calibrated tapered tube flowmeters. Pressure was measured using Dwyer Instrument Series 2000 Magnehelic pressure gages immediately downstream of the flowmeters. Temperature was measured in the manifolds utilizing copper-constantan thermocouples. Manifolds were numbered as shown in Figure 2.3 and data recorded for each manifold separately.

2.3 Arrangement

Figure 2.4 shows the basin layout used to accomplish the tests. The model was first tested on the East Side of the model basin and then moved to the West Side. The airflow and velocity conditions tested in solid ice were repeated in brash.

2.4 Model Scaling Laws

For model testing to be correct, the model must be both geometrically similar and dynamically similar to the full-scale prototype. The first is achieved by scaling all dimensions by the geometric scale factor λ . The second condition is achieved by maintaining the ratio of significant forces the same for both the model and the prototype.

In testing a ship model in ice, the significant forces are gravity forces, dynamic forces, ice forces, and friction forces. Gravity forces will scale by λ^3 since the density of water is the

TABLE 2.1 SHIP AND MODEL DATA

for
140 FT. WYTM

Model No. 202C

APPENDAGES : Rudder and Bubbler Duct

LINES DWG NO.: 140-WYTM-0101-1
ALT D

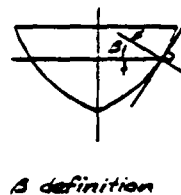
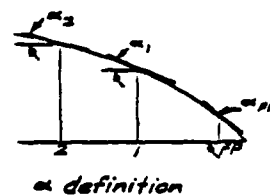
DIMENSIONS		
ITEM	SHIP	MODEL
Length (LOA), m	42.67	1.778
Length (LWL), m	39.62	1.651
Length (LBP), m	39.62	1.651
Beam, Max (at LWL), (B_x), m	10.41	0.434
Beam, Max, m	11.43	0.476
Draft (at test WL), m	3.658	0.152
Trim (test) (+ AFT), m	0	0
Displacement, Metric Tons	673	0.0487
Wetted Surface Area, Sq. m	409	0.710
Distance from FP to B_x , m	21.79	0.908
Distance from B_x to LCF (+ AFT), m	-1.393	-0.058
Distance from B_x to \overline{CG} (+ AFT), m	-1.981	-0.083
Distance from LCG to \overline{CG} (+ AFT), m	-0.710	-0.030
Longitudinal Metacenter Above Keel, m	5.15	0.215

COEFFICIENTS AND ANGLES (AT TEST WL)

Block Coefficient	0.437	Length/Beam	3.81
Midship Section Coefficient	.748	Beam/Draft	2.85
Prismatic Coefficient	.589	μ_0	1.44
Waterplane Coefficient	.715	η_2	3.03
Bow Stem Angle, Deg.	30°	λ	24
Half Entrance Angle, Deg.	27°		

TABLE 2.1 (CONTINUED)

Item Station	B_i/B_n	α_i	β_i
0	0	28.3°	48.0°
1	.204	26.5°	43.5°
2	.388	23.5°	42.5°
3	.537	20.3°	39.0°
4	.670	16.5°	35.0°
5	.775	13.5°	30.5°
6	.857	10.5°	27.0°
7	.917	7.5°	25.0°
8	.958	5.0°	22.2°
9	.983	3.0°	19.7°
10	.996	1.0°	18.5°
11	1.000	0°	19.0°
12	.997	-1.0°	19.2°
13	.984	-3.3°	20.0°
14	.950	-7.5°	23.5°
15	.886	-12.0°	27.5°
16	.787	-17.3°	35.3°
17	.653	-22.2°	44.5°
18	.482	-27.0°	54.5°
19	.272	-31.0°	62.2°
20	0	-33.0°	72.7°



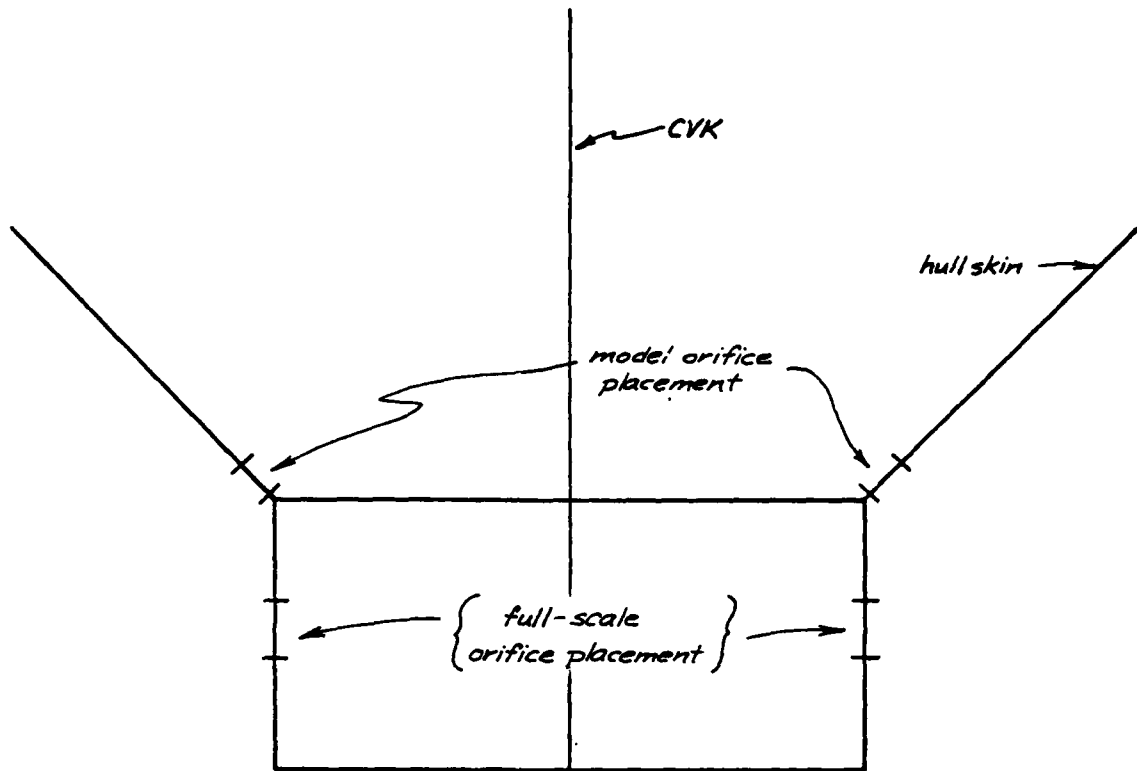


Figure 2.2. Bow Manifold Orifice Placement

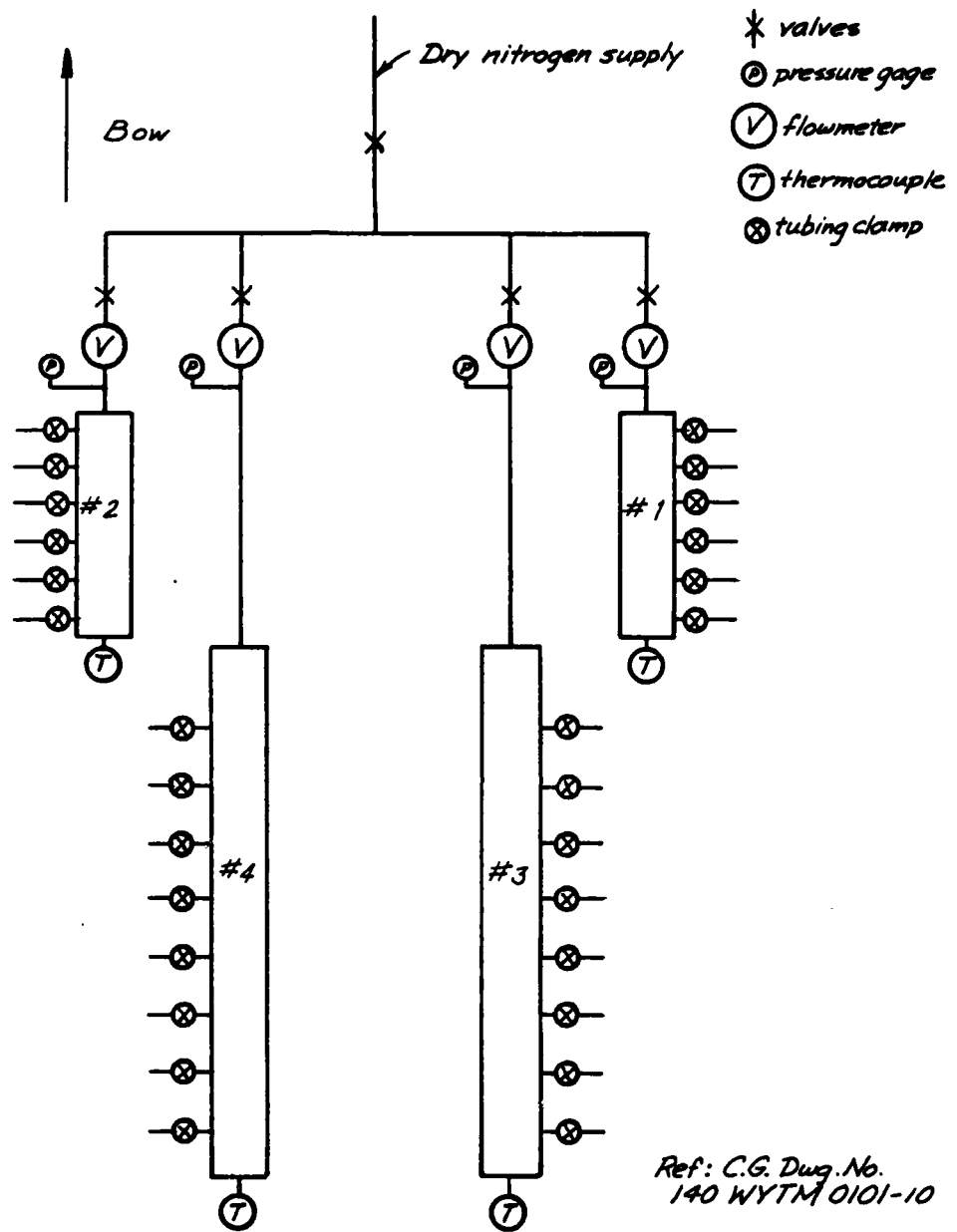


Figure 2.3. Bubbler System Schematic

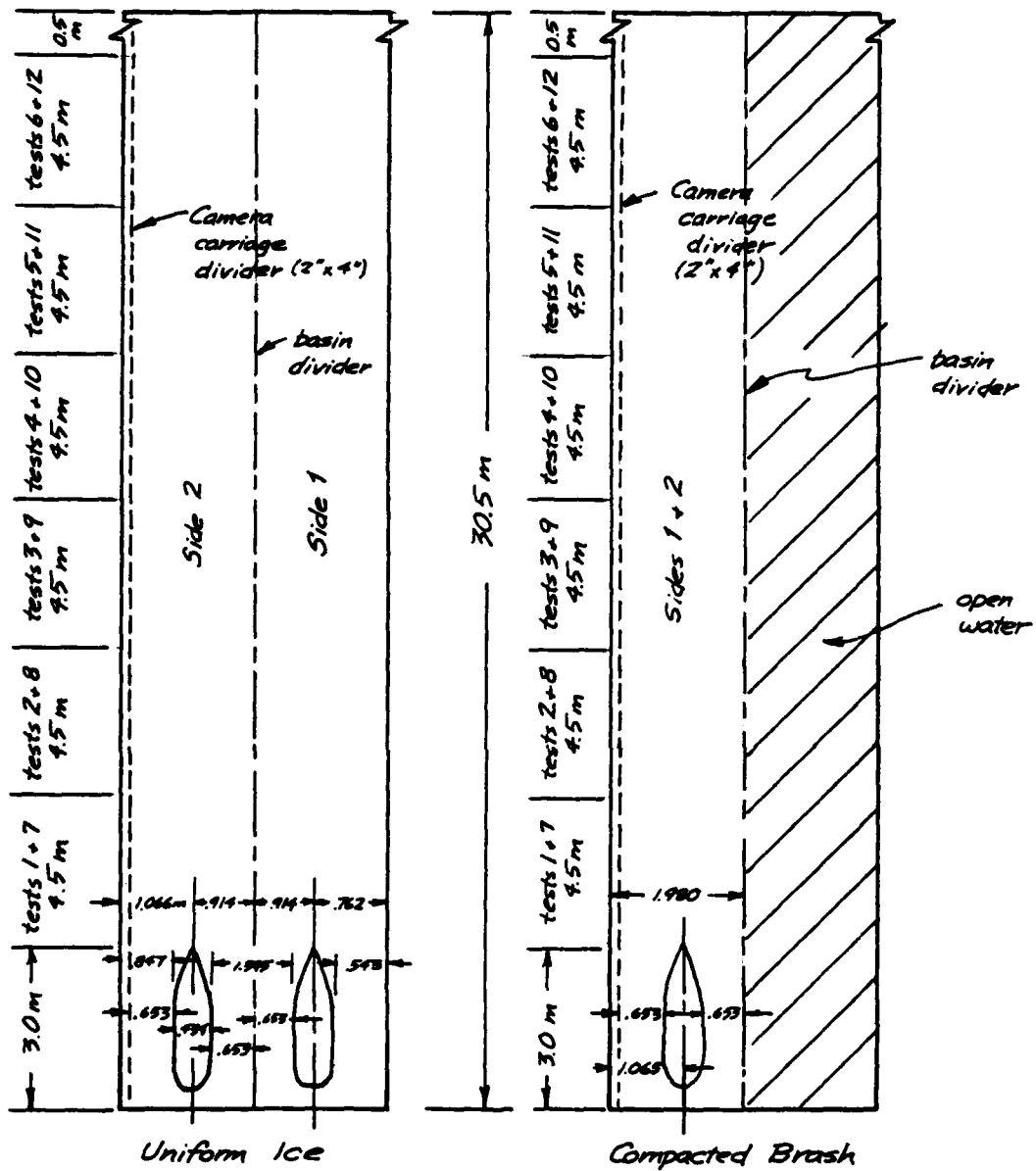


Figure 2.4. Basin Layout

same for both the model and the full-scale ship. It then follows that the dynamic forces must also scale by λ^3 , which is achieved by testing the model at speeds corresponding to the full-scale speeds divided by $\sqrt{\lambda}$. This results in the Froude number v/\sqrt{gL} being the same for both the model and the prototype.

From the principle that all forces acting on the model must scale by λ^3 , the scaling laws listed in Table 2.2 can readily be derived. These laws dictate that the model ice thickness h , flexural strength σ_f , and elastic modulus E must be reduced from the appropriate full-scale values by the scale factor λ , and the density of ρ_i must be equal to the full-scale value. Bubbler scaling laws are discussed in Appendix E.

In using this procedure, the viscous forces do not scale properly. These forces, however, will be negligibly small compared to the other forces involved.

2.5 Model Testing Facility

The model test series was conducted in the ARCTEC Ice Model Basin, Columbia, Maryland. This facility consists of a refrigerated model towing basin 30.5 metres long, 3.7 metres wide, and 1.5 metres deep, which is filled with a saline solution. On the surface, ice is frozen to a thickness equal to the geometric scale of the desired full-scale ice thickness. By controlling the water salinity, freezing rates, and temperatures, model ice is produced with properties correctly scaled for model testing, with the exception of the elastic modulus.

The models are towed through the ice sheet at constant speed and the resistance is measured. The carriage drive system is capable of towing at any desired model speed.

2.6 Resistance Test Procedure

The two test tracks were arranged side-by-side in order to obtain the greatest number of data points from each ice sheet. This procedure has been shown to be valid providing the distance between the models is greater than six characteristic lengths and the distance from the models to the basin walls is greater than three characteristic lengths [1]. For this criterion, the characteristic length l_c of the ice is defined by:

$$l_c = \sqrt[4]{\frac{Eh^3}{12\rho_w g}} \quad (2.1)$$

TABLE 2.2 SCALING LAWS FOR MODELING*

<u>Variable</u>	<u>Symbol</u>	<u>Scaling Law</u>
Length	L	$L_{fs} = \lambda L_{ms}$
Beam	B	$B_{fs} = \lambda B_{ms}$
Ice Thickness	h	$h_{fs} = \lambda h_{ms}$
Ice Flexural Strength	σ_f	$\sigma_{ffs} = \lambda \sigma_{fms}$
Ice Elastic Modulus	E	$E_{fs} = \lambda E_{ms}$
Speed	v	$v_{fs} = \sqrt{\lambda} v_{ms}$
Time	t	$t_{fs} = \sqrt{\lambda} t_{ms}$
Resistance	R	$R_{fs} = \lambda^3 R_{ms}$
Mass	M	$M_{fs} = \lambda^3 M_{ms}$
Mass Moment of Inertia	I	$I_{fs} = \lambda^5 I_{ms}$
Mass Density of Water	ρ_w	$\rho_{wfs} = \rho_{wms}$
Mass Density of Ice	ρ_i	$\rho_{ifs} = \rho_{ims}$
Coefficient of Kinetic Friction	f	$f_{fs} = f_{ms}$
Volume Flow	Q	$Q_{fs} = \lambda^{2.5} Q_{ms}$
Power	P	$P_{fs} = \lambda^{3.5} P_{ms}$

* Subscripts fs = full-scale
ms = model-scale

where

- E = elastic modulus of the ice sheet
- h = thickness of the ice sheet
- ρ_w = mass density of water
- g = acceleration due to gravity

The ratio d/l_c (where d is the distance from the side of the model to the basin wall) must exceed 3. Thus, maximum ice thickness for dual model tests is:

$$h_{\max} = \sqrt[3]{\frac{12 \rho_w g l_c^4}{E}} = 31.7 \text{ mm.}$$

where:

- $E = 4 \times 10^6 \text{ N/m}^2$ (Approximate actual basin value, not correctly scaled)
- $\rho_w = 1005 \text{ kg/m}^3$
- $g = 9.807 \text{ m}$
- $d = 543 \text{ mm}$ (see Figure 2.4)

All tests met this criterion. By using approximately two model-lengths per data point, the models could be towed at six different velocities in each ice sheet, thereby collecting twelve data points per ice sheet.

For each test the speed v of the towing carriage and the resistance R of each model were recorded on an oscillograph. In addition, the flexural ice strength σ_f was measured in three locations before and after each track. The elastic modulus E was measured at three positions prior to each track, and the ice thickness was measured every metre on both sides of the broken channel following the test run. The throttling valves ahead of the flowmeter were adjusted until test values of flow existed. Table 2.3 contains a list of test values. After two ice sheets, the lowest two values were added and the highest two dropped when there appeared to be little change with the highest flows. Gas temperature and pressure were measured to correct this flow to standard conditions before conducting the data analysis. The equation used to correct flowmeter reading was:

$$Q_s = \left[\left(\frac{p_N}{p_s} \right) \left(\frac{T_s}{T_N} \right) \left(\frac{R_N}{R_{\text{air}}} \right) \right]^{1/2} Q_R \quad (2.1)$$

TABLE 2.3 TARGET AIR FLOWS UTILIZED

Name	Full-Scale ft ³ /min	Model-Scale ft ³ /h	Bow Man. ft ³ /h	Amidships Man. ft ³ /h
Q ₀	-----	NO FLOW	-----	-----
Q _{4B}	938	20.0	4.5	5.5
Q _{3A}	1,875	39.9	9.0	10.9
Q ₁	3,750	79.8	18.1	21.8
*Q ₂	7,500	159.5	36.1	43.6
Q ₃	11,250	239.2	54.2	65.4
Q ₄	15,000	319.0	72.2	87.2

* Design

where:

- Q_S = flow at standard conditions
- Q_R = flowmeter volume (instrument error removed)
- P_N = nitrogen pressure
- P_S = standard pressure = 14.7 psia = 407 in. H₂O
- T_S = standard temperature = 289°K = 520°R
- T_N = nitrogen temperature
- R_N = nitrogen gas constant = $55.1 \frac{\text{ft. lb(f.)}}{(\text{lb(m)})^\circ\text{R}}$
- R_{air} = gas constant for air = $53.3 \frac{\text{ft. lb(f.)}}{(\text{lb(m)})^\circ\text{R}}$

All data is tabulated in Appendix A.

The resistance of the model was measured using a strain-gaged force block. The model was attached to the force block in such a way to allow pitching, rolling, and heaving motions. The models were restrained in yaw and sway. A daily calibration of the force block was performed in order to ensure accurate measurements.

The model speed and position were measured simultaneously by recording the passing of six spokes in a wheel of the carriage drive system. Each pulse on the oscillograph indicates a carriage movement of a fixed distance. By recording the distance traveled on a time-based recorder, the velocity can be calculated. The carriage position in relation to the ice sheet was determined by noting the starting position of the models and then counting the pulses.

High-speed underwater movies were taken at a frame speed of $24\sqrt{\lambda}$ frames per second. When projected at normal speed, the motion of the model is viewed in full-scale time. Supplemental surface footage was taken with a normal speed camera. Test films were edited, spliced together, and titled to produce a film summary of the program.

2.7 Brush Preparation and Monitoring

After testing in level ice, the ice sheet was broken up into small, random size pieces of which 50% were less than 25 mm on the largest dimension. The broken ice was compacted into an area of even thickness of 30 to 45 mm corresponding to an average full-scale thick-

ness of 3 feet. Thickness was measured using the gage shown in Figure 2.5. This modeled unconsolidated brash ice. In order to further characterize the model brash ice, two additional measurements were made.

The first was made with a cone penetrometer. This consisted of a weighted cone made of transparent plastic with a 40° angle. Graduations for depth of penetration were marked on the inside of the cone. This was used primarily to ensure that the brash ice was of uniform compactness. Figure 2.6 shows the cone penetrometer.

The second measurement determined the mass of ice per unit volume. This was made using a wire basket (300 x 300 x 100 mm) to lift the ice out of the water. After it was allowed to drain, the weight of the ice in the basket was measured using a shipping scale.

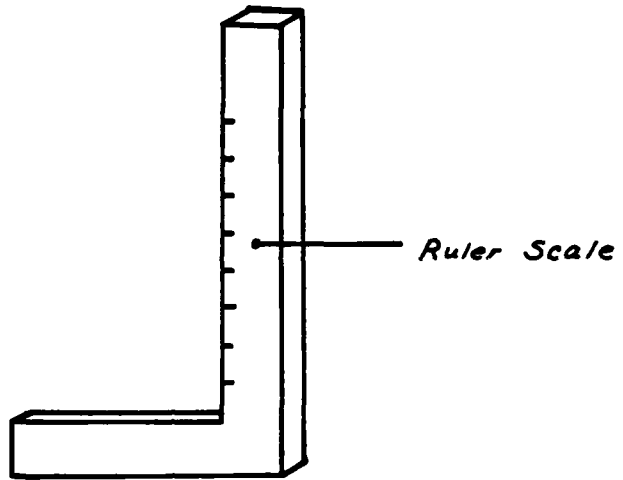


Figure 2.5. Brash Thickness Measuring Device

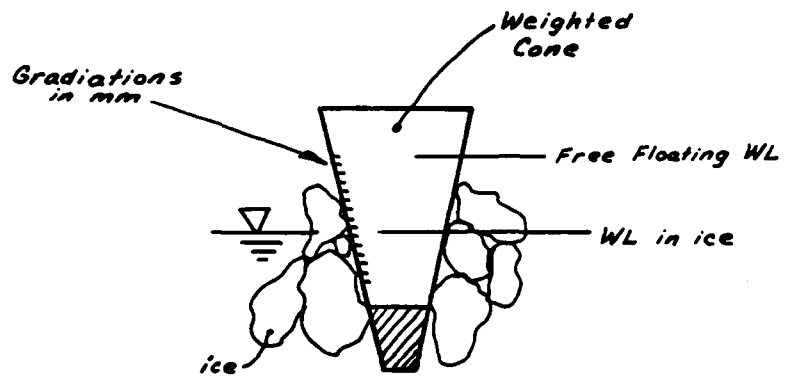


Figure 2.6. Cone Penetrometer

3. RESULTS

3.1 Resistance Data

All of the resistance data collected during the tests is contained in Appendix A. There are three sections to Appendix A. The first section contains the resistance data using the units in which it was measured at the model scale. The second section of Appendix A contains the same data; however, the data has been formed into dimensionless groups for the purpose of analyzing and comparing resistance obtained in this series with earlier series results and eliminating the effects of variations in thickness from test to test. The third section of Appendix A contains the data scaled-up using the scaling laws in Table 2.2 to reach values of resistance and velocity, etc., for each individual data point as they would pertain to the actual tug. Table 3.1 contains conversion factors from English to SI Units.

The model data is listed in SI units. This system was commonly known as the metre kilogram second system up to 1960. The resistance is thus measured in newtons, the velocity in millimetres per second, the thickness of the ice in millimetres, the strength of the ice in kilopascals, the pressure in the manifolds is in pascals, and the temperature measured in the manifolds in degrees celsius. The volume flow rate is given in cubic metres per hour, while the power is given in watts. The volume flow has been calculated for standard conditions using Equation 2.1, which is repeated here.

$$Q_s = \left[\left(\frac{p_N}{p_s} \right) \left(\frac{t_s}{T_N} \right) \left(\frac{R_N}{R_{air}} \right) \right]^{1/2} Q_R \quad (2.1)$$

The compressor power necessary to obtain this volume flow rate is calculated using a compressor efficiency of 0.7 and the equation for isentropic compression of air is as follows:

$$W = \frac{k p_1 V_1}{k-1} \left[\left(\frac{p_2}{p_1} \right)^{\frac{k-1}{R}} - 1 \right] \quad (3.1)$$

where:

- W = work
- k = ratio of specific heats, 1.4 for air
- p_1 = initial pressure
- p_2 = outlet pressure
- V_1 = inlet volume
- R = gas constant for air

Pressure at the air compressor on the tug itself has been calculated from the volume flow rate using the actual piping system performance

TABLE 3.1 CONVERSION FACTORS

<u>To Convert From</u>	<u>To</u>	<u>Multiply By</u>
long tons	kN	9.962
ft	m	0.3048
knots	m/s	0.5144
lbf/in ²	kPa	6.895
ft ³ /min	m ³ /s	4.719x10 ⁻⁴
HP	watts	746.0

as calculated in the design manual which is Reference 2. This manual contains performance curves of volume flow rate versus pressure at the compressor.

The dimensionless groups which were used in this program were those which have been developed using long standing practice at ARCTEC. The quantity of data available at any single condition of the hull or bubbler system is too small to allow the empirical formation of different dimensionless groups. One main purpose of dimensionless groups is to reduce the number of variables present such that the analysis can be more efficiently conducted. The single variable which effects the performance most is the thickness of the ice; therefore, each dimensionless group contains the thickness of the ice raised to some power within it. Figure 3.1 shows a plot of the dimensionless resistance versus the product of dimensionless strength and dimensionless velocity. These two terms were found to be the most important in explaining the variation in resistance found in the earlier WYTM tests. All of the data obtained during this test program in solid ice is plotted in Figure 3.1 using these two dimensionless variables. A look at the data indicates that there is a large amount of scatter present and that no direct conclusions are possible by simply looking at the way the data falls. In brash ice, previous experience leads to the formation of two different dimensionless groups to explain the variation in resistance which is seen. The first dimensionless group or dimensionless brash resistance is the resistance measured divided by the weight density of ice times the beam of the model and thickness of the brash field squared. The dimensionless velocity squared is the term against which this resistance is plotted. It can also be seen from an examination of the plot in Figure 3.2 that a readily made conclusion is not possible on the performance of the tug in brash due to the large scatter in the data.

We can, however, compare the results which were obtained in this series of tests without the bubbler system operating with those which were obtained using the sanded hull form during the earlier tests of the 140-FT. WYTM. Data which falls within the range of data gathered during this series is plotted on Figure 3.3. A separate regression equation was developed for the tests conducted earlier in only 1-1/2 feet of ice. This line is also plotted on Figure 3.3. Along with the data collected during these tests, we have plotted a regression of the performance of the tug without the bubbler system also. From this it can be seen that in spite of the fact that a lower hull-ice friction was measured in this series, the resistance was somewhat higher at all speeds tested than for the earlier tests. However, we can also see that the scatter of the data is such that all of the data points collected both before this series and during this series fall within the same band, and thus represent the same group. The error or mismeasurement of the resistance appears to vary from approximately 10% at zero speed to 33% at 5 knots.

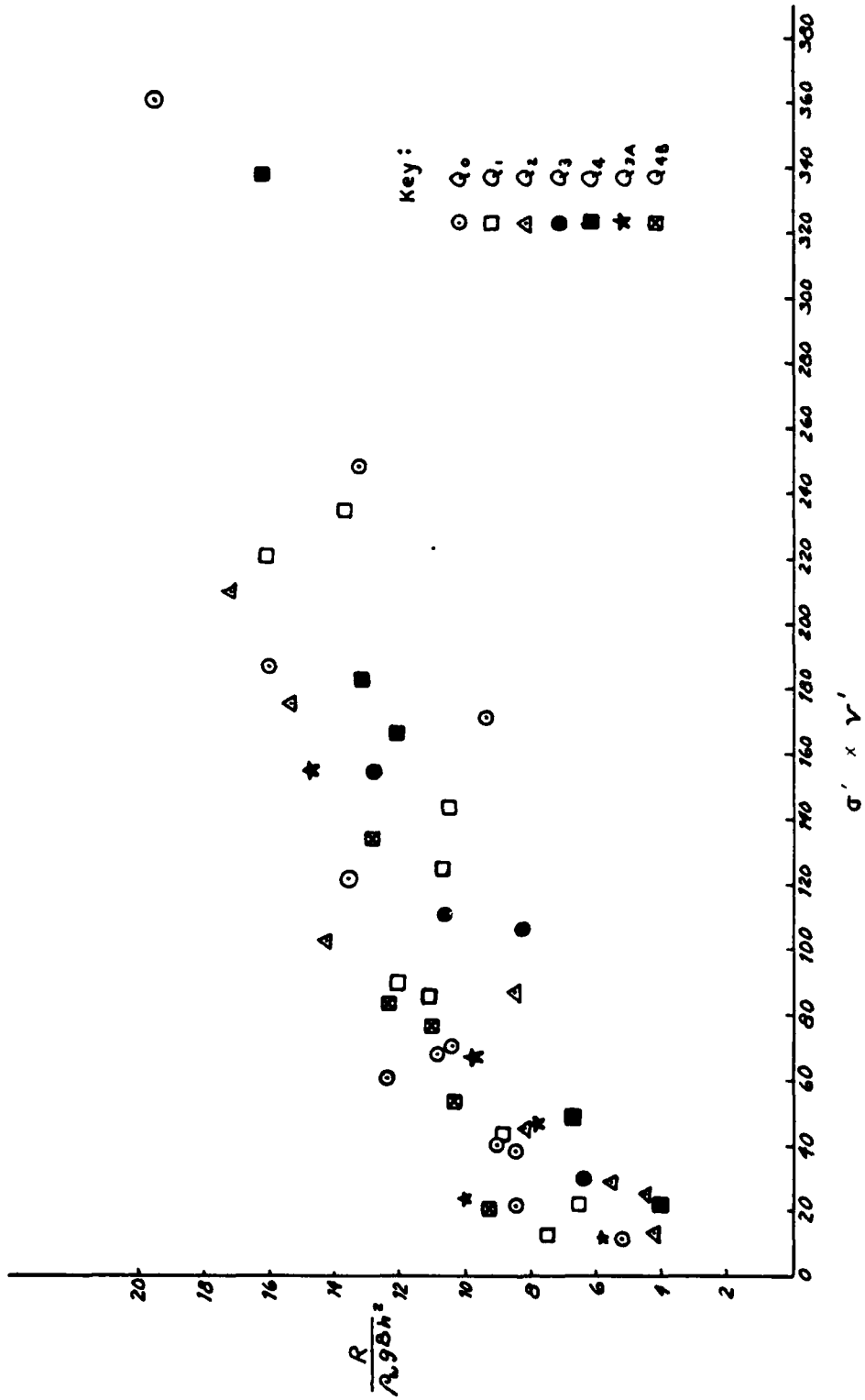


Figure 3.1 : Dimensionless Resistance - Solid Ice

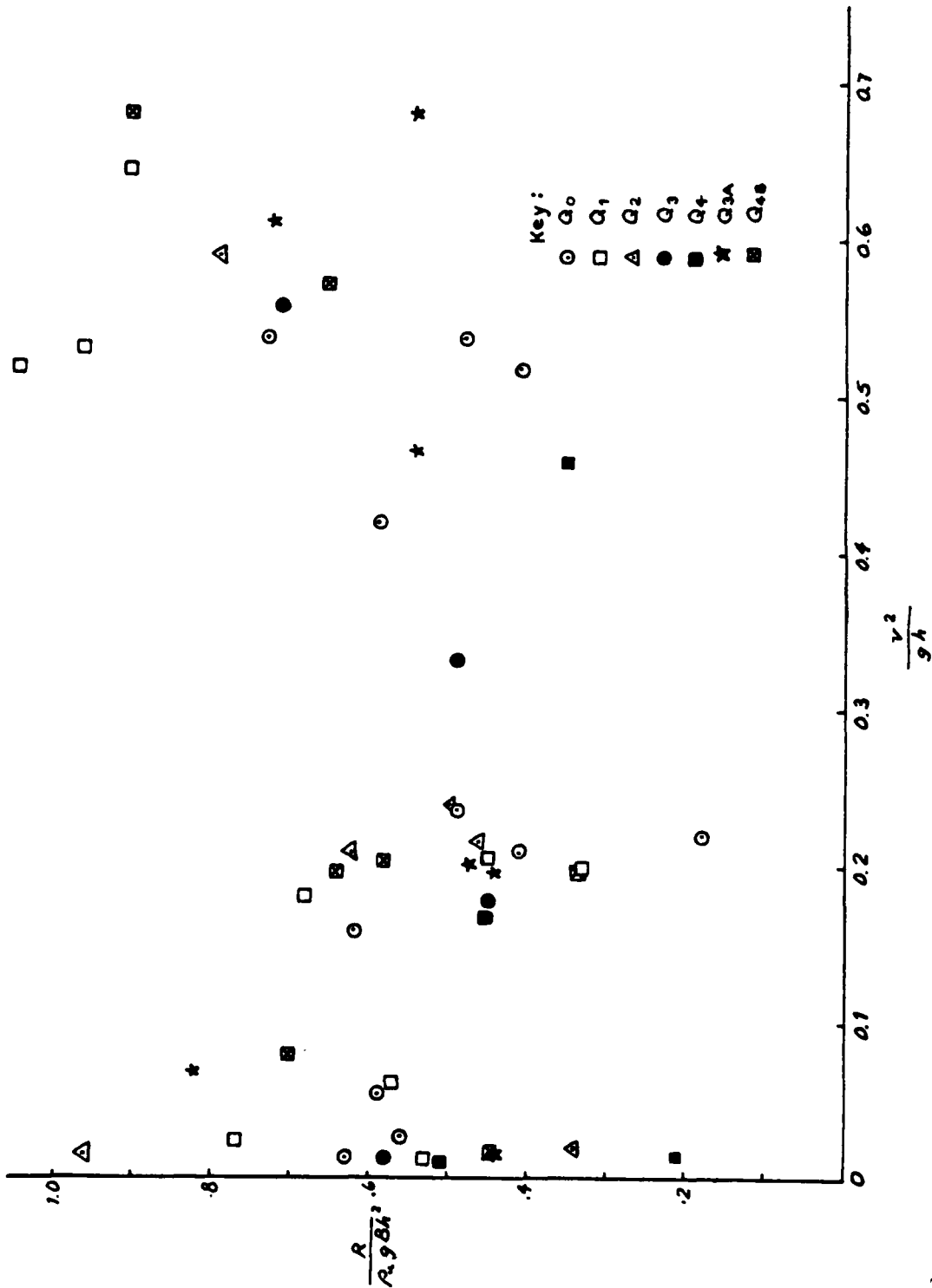


Figure 3.2 : Dimensionless Resistance - Brash Ice

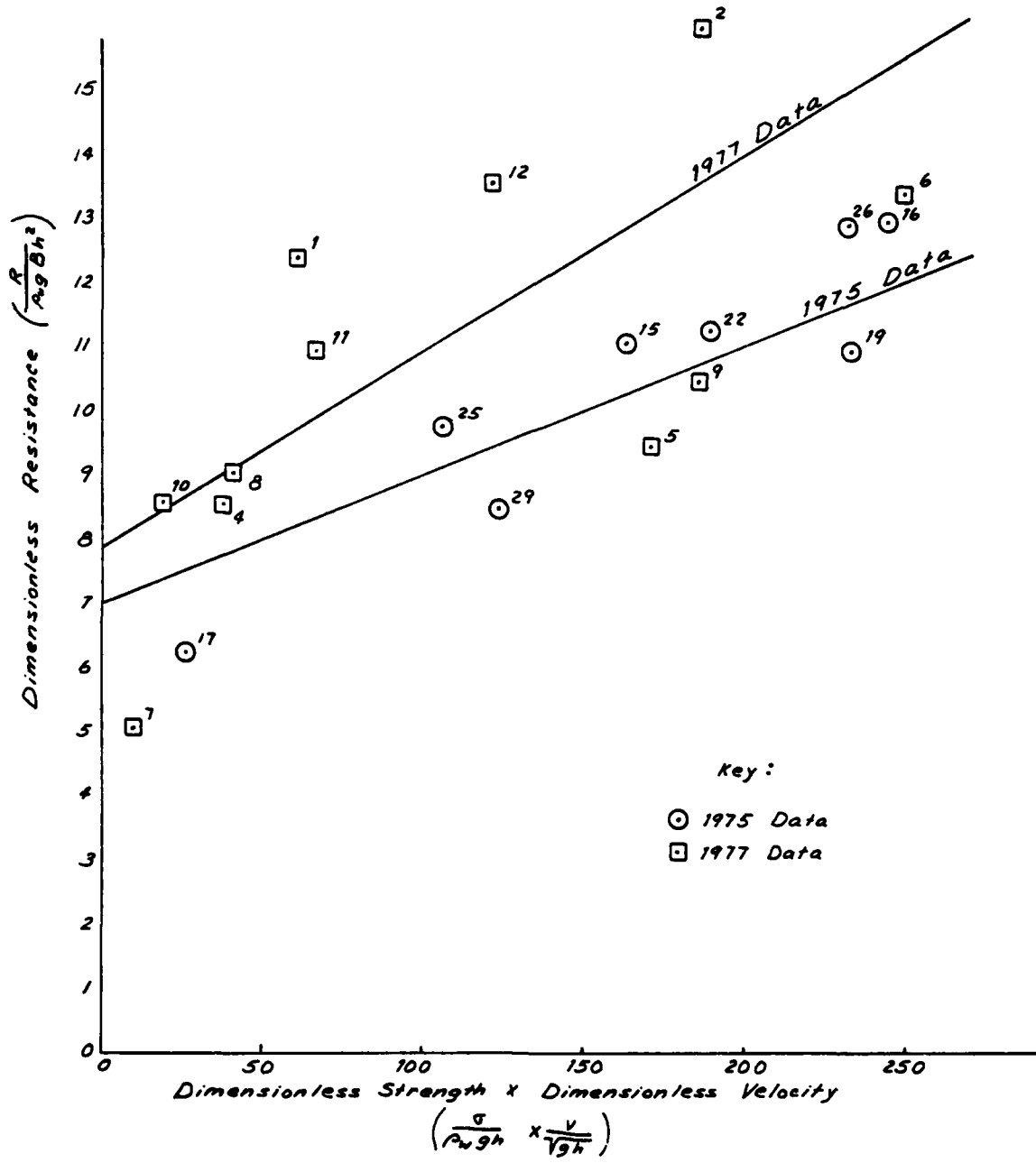


Figure 3.3: Comparison of Results Without Bubbler With 1975 Tests

3.2 Friction Data

The hull-ice friction was measured at four locations on the hull of the 140-FT. WYTM Model. The friction was measured many times at each of the four locations and this data is recorded in Appendix B. The average of all the friction tests was 0.232.

3.3 Ice Data

The properties of the model ice are contained in Appendix C. The strength given in this particular tabulation is the average of the strength for all data points obtained in solid ice during a given day, thus, it may not correspond exactly to the strength recorded for individual data points. In the analysis, individual strengths were used for each data point. In the brash data, it should be noted that the density of ice to water within the brash sheet was approximately 0.65.

4. ANALYSIS

4.1 Tug Performance in Open Water

Thrust curves for the actual propeller to be utilized and the actual hull form for the WYTM were obtained using the data contained in Reference 5. The $1-t$ value of 0.81 and the $1-W_T$ value of 0.745 tested at 5 knots were assumed to hold constant down to the bollard. The propeller thrust was calculated from the Equation:

$$T_P = \frac{K_T \rho_w \dot{h}^2 D^4 (1-t)}{2240} = 3.66 K_T n^2 \text{ in long tons} \quad (4.1)$$

While the ship velocity at various J-factors was calculated using this following equation:

$$V_K = \frac{nDJ}{1.688(1-W_T)} = 6.76nJ \text{ in knots} \quad (4.2)$$

Open water resistance was calculated using the following equations and the values for estimated horsepower tabulated in the David Taylor Model Basin tests.

$$R_{OW} = \frac{550 \cdot \text{EHP}}{V_K 1.688} \text{ in long tons} \quad (4.3)$$

The curves were constructed for five values of constant shaft horsepower varying from the bollard to about 5 knots. The results of these calculations are presented in Figure 4.1 which is a re-presentation of the actual performance of the WYTM with its installed power for intermediate values of horsepower up to full power on the shaft. Also, plotted on this figure are the open water resistance and three additional power levels which are sketched in above the capability of the installed propulsion plant, for the purpose of evaluating some of the solid ice resistance data at 5 knots which was much higher than the capabilities of the present ship.

4.2 Continuous Motion Through Solid Ice

In this section we will discuss the results which were obtained for towing the ship at constant speed through solid ice with and without the air bubbler system in operation. The data from Appendix A was placed into a file on the computer and submitted to a forced fit to

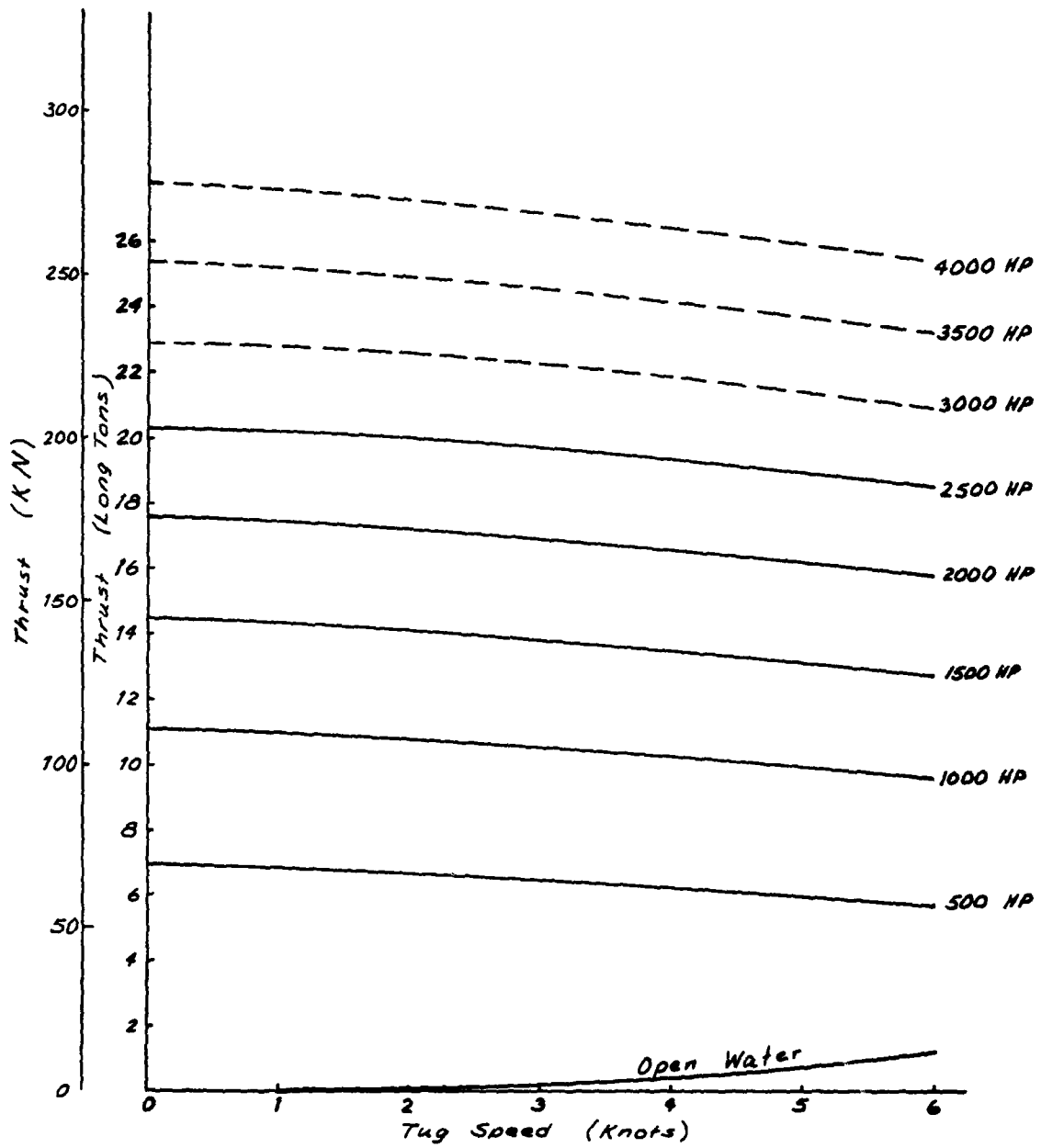


Figure 4.1 : Propeller Thrust Behind 140 ft WYTM Hull

the following two equations:

$$\frac{R}{\rho_w g B h^2} = C_0 + C_1 \left(\frac{\sigma_f}{\rho_w g h} \right) \left(\frac{v}{\sqrt{g h}} \right) \quad (4.4)$$

$$\frac{R}{\rho_w g B h} = C_2 + C_3 \left(\frac{v}{\sqrt{g h}} \right) \quad (4.5)$$

The results of this regression analysis are tabulated in Table 4.1 which contains the regression coefficients for resistance in solid ice. The first column in this table contains the setting names which pertain to the settings or division of air flow to the bow and the midships manifold given in Table 2.3. The second column is the volume flow in standard cubic feet per minute, full-scale corrected for the temperature and pressure of the gas utilized during the tests. The third column is the full-scale compressor power required based on the existing WYTM piping system and the pressure drop associated with that system as calculated in the design report, Reference 2. The fourth, fifth, and sixth columns in this table are the mean values of the variables which were subjected to regression for each of the conditions tested. The regression solution always forces the regression line through the mean value of all the data, therefore, the line Equation 4.4 must pass through the mean value of $R/\rho_w g h^2$ at the mean value of:

$$\left(\frac{\sigma_f}{\rho_w g h} \times \frac{v}{\sqrt{g h}} \right)$$

while equation 4.5 must utilize the mean value of $R/\rho_w g B h^2$ and the mean value of $v/\sqrt{g h}$. Computer print-outs for these fits are found in Appendix D. The coefficients that were determined by the regression solution are then tabulated in the next four columns listed C_0 , C_1 , C_2 and C_3 . The number of data points which were available for each regression are tabulated in the last column. Because of the small number of data points, the value for the multiple correlation coefficient for these regression equations was quite poor. However, the fit to the first equation, Equation 4.4, was much better than the fit to Equation 4.5. Also, as can be seen by a cursory examination of the coefficients, the agreement between the different flow rates is much better when the strength effect is taken into consideration, as it is in Figure 4.4, than when it is not as in Equation 4.5.

TABLE 4.1 REGRESSION COEFFICIENTS FOR REGRESSION IN SOLID ICE

Setting Name	Vol.* ft ³ /m	Power HP	$\frac{R}{\rho_w g B h^2}$ mean	$\frac{v}{\sqrt{gh}}$ mean	$\left(\frac{\sigma}{\rho_w g h} \times \frac{v}{\sqrt{gh}} \right)$ mean	C ₀	C ₁	C ₂	C ₃	No. of Points
Q ₀	0	0	11.40	.6233	116.7	7.82	.0307	7.19	6.75	12
Q _{4B}	1,000	28	11.13	.718	74.3	8.72	.0324	8.52	3.63	5
Q _{3A}	2,000	57	9.62	.602	60.5	6.39	.0534	6.40	5.35	5
Q ₁	4,000	118	10.77	.631	108.7	7.14	.0334	6.48	6.79	9
Q ₂	8,000	283	9.74	.588	86.1	3.97	.0671	2.94	11.58	8
Q ₃	12,250	567	9.55	.655	100.8	4.48	.0502	5.11	6.76	4
Q ₄	16,800	1,020	10.48	.650	151.7	4.72	.0379	4.66	8.94	5

*Target values corrected to actual test conditions for use of nitrogen gas, gas temperature, and pressure at the flowmeter.

The coefficients C_0 and C_1 were then plotted against volume flow on Figure 4.2. The slopes for Q_{3A} , Q_2 , and Q_3 are omitted from the figure because they appeared to be abnormally high. A line passed through the slopes for Q_0 and Q_1 (those points containing the most data) passes near the slopes of Q_{4B} and Q_4 . This line was used to obtain "faired" values of slope, C_1 , for the remainder of the analysis. The corresponding value of intercept, C_0 , to pass a line through the mean of each flow setting data set is then calculated in the next column of Table 4.2. The second intercept values are also plotted in the lower half of Figure 4.2 and a line drawn through them. The values along the line were then read off and a smooth family of resistance curves is thus obtained such that the mean for the family goes through the mean of the raw data. This family of dimensionless resistance curves is plotted in Figure 4.3. Also plotted in Figure 4.3 are the thrust curves for the tug when the resistance curves represent 1-1/2 feet of 126.5 psi ice. The dimensionless coefficients could be used to calculate the resistance in any other thickness of ice desired. The power required for the tug to proceed through 1-1/2 feet of ice was then evaluated at 1, 3 and 5 knots. The results of this evaluation are contained in Figures 4.4 through 4.6. This is plotted as the required horsepower at this speed through 1-1/2 feet of 126.5 psi ice. The value of 126.5 psi is the mean value of ice strength encountered during the tests of the icebreaker MACKINAW on the Great Lakes. The solid line on each of these curves is the compressor horsepower required to produce the volume flow through the existing piping system on the WYTM. If the piping system were resized and optimized for each particular flow rate, the pressure drop would remain constant and this line would become straight as shown by the dashed line on Figure 4.4. Since 7,500 scfm is the design point, a straight line through the 7,500 scfm power point and the origin would be the characteristic of the compressor power curve under these conditions. The shaft horsepower curve is extracted from the predictor equations and their intercept with the propeller characteristics. The total power is then the sum of compressor power and shaft horsepower. The lowest point on the total power curve corresponds to the point of optimum operation of the bubbler system for that particular speed.

4.3 Continuous Motion Through Brash Ice

The continuous motion through brash ice data contained in Appendix A was formed into dimensionless groups corresponding to the groups in the following equation:

$$\frac{R}{\rho_i g B h^2} = C_4 + C_5 \left(\frac{v^2}{gh} \right) \quad (4.6)$$

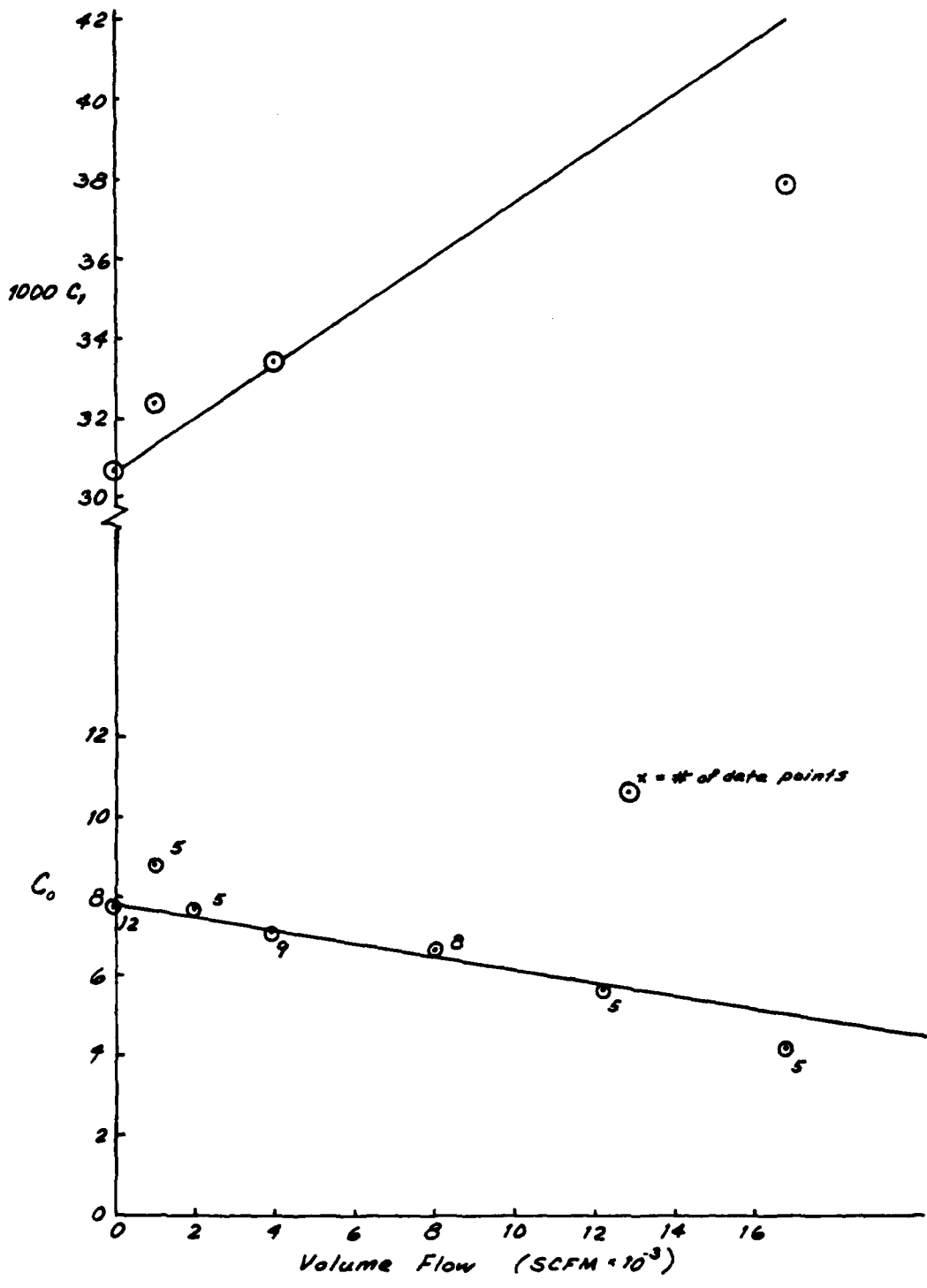


Figure 4.2 : Solid Ice Predictor

TABLE 4.2 PREDICTOR FOR SOLID ICE

Setting Name	Vol. ft ³ /m	C_1 estimated	C_0^*	C_0 estimated
Q_0	0	.0307	7.82	7.82
Q_{4B}	1,000	.0314	8.80	7.63
Q_{3A}	2,000	.0321	7.68	7.45
Q_1	4,000	.0334	7.14	7.19
Q_2	8,000	.0361	6.63	6.50
Q_3	12,250	.0390	5.62	5.80
Q_4	16,800	.0420	4.11	5.05

$$*C_0 = \left(\frac{R}{\rho_w g B h^2} \right) \text{mean} - (C_1) \text{ estimated} \times \left(\frac{v}{\sqrt{gh}} \times \frac{\sigma}{\rho_w g h} \right) \text{mean}$$

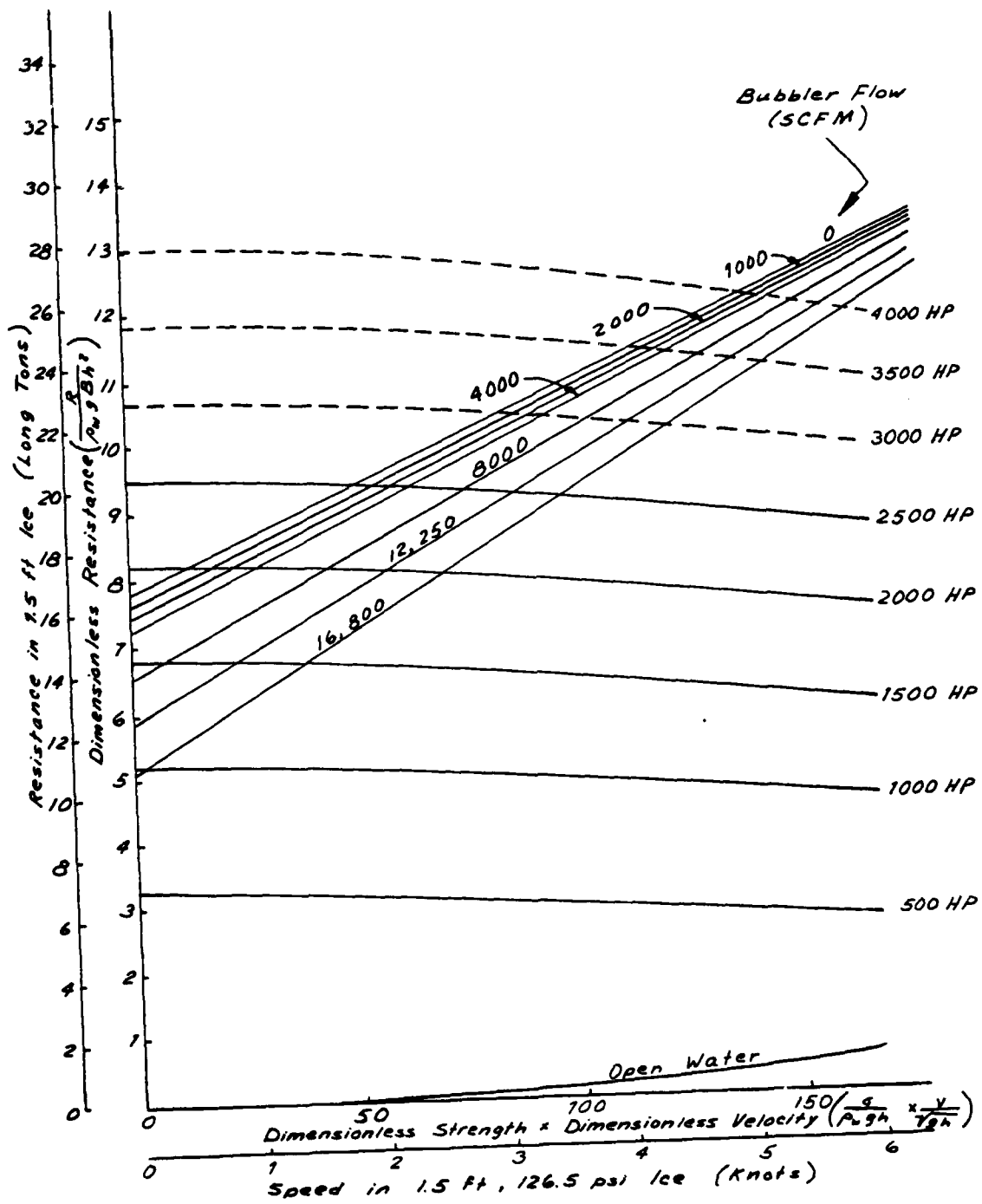


Figure 4.3 : Tug with Bubbler in 1.5 ft Solid Ice

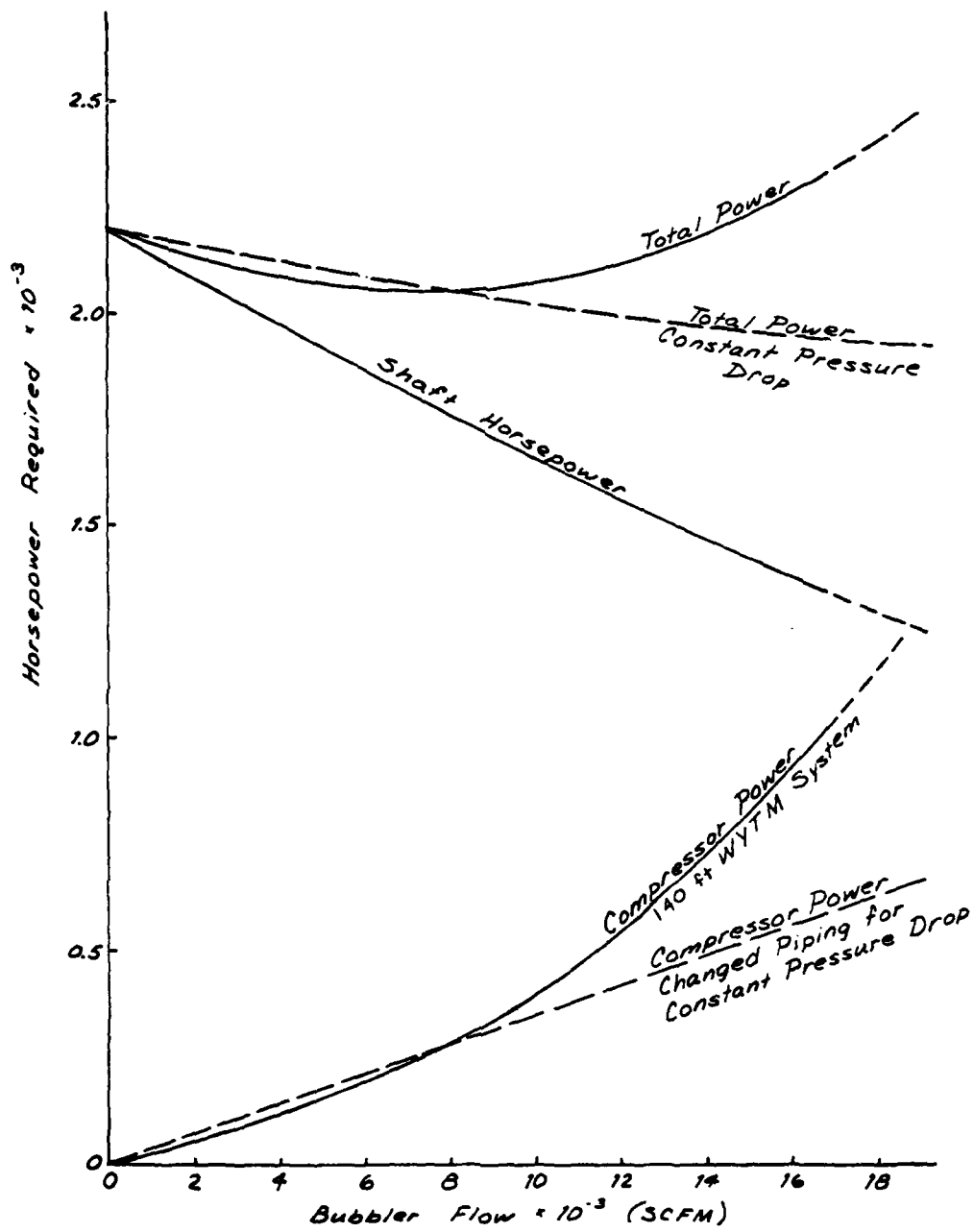


Figure 4.4: Bubbler Performance at 1 Knot in 1.5 ft Solid Ice of 126.5 psi Strength

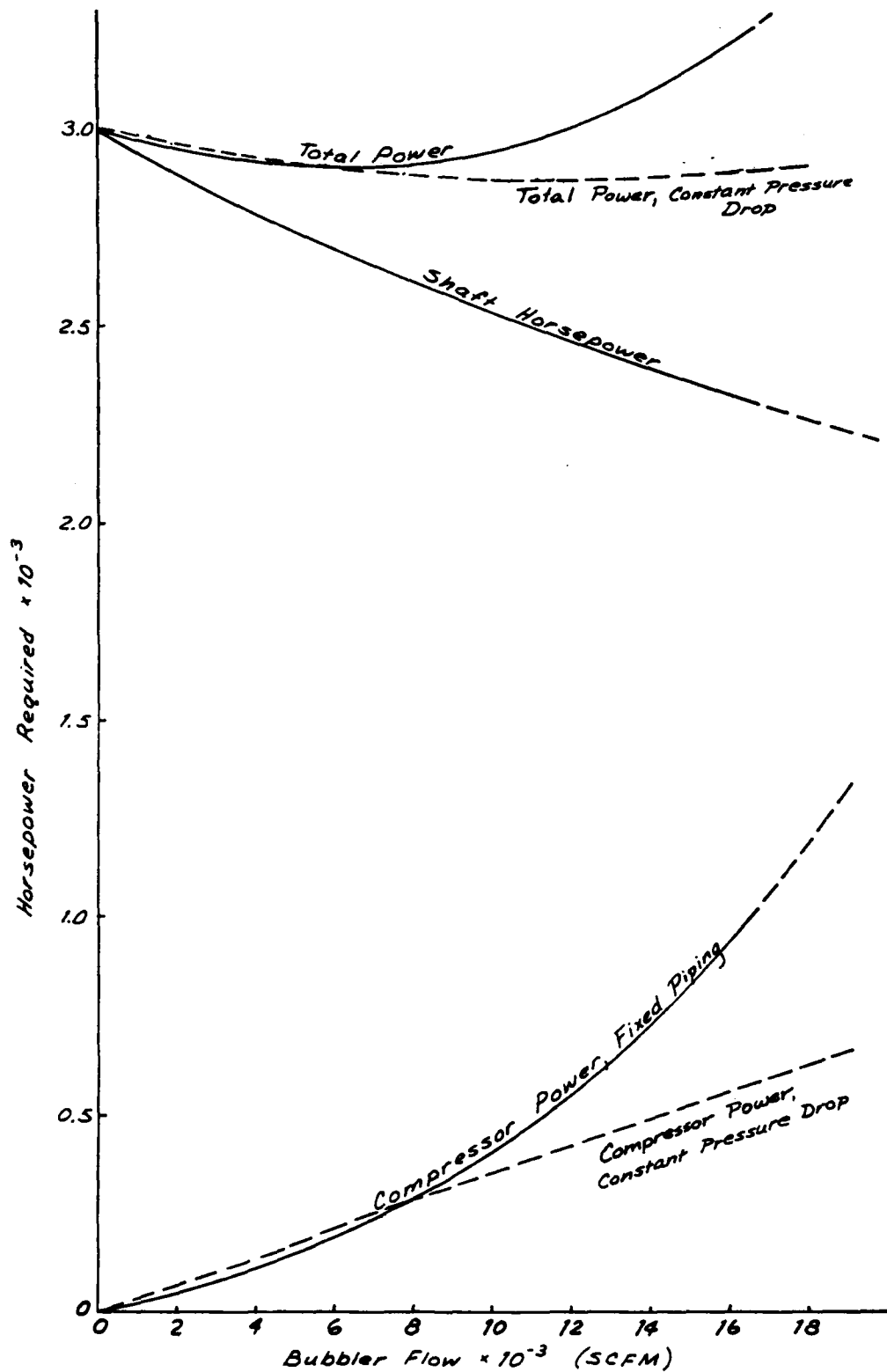


Figure 4.5: Bubbler Performance at 3 Knots in 1.5 ft of 126.5 psi Solid Ice

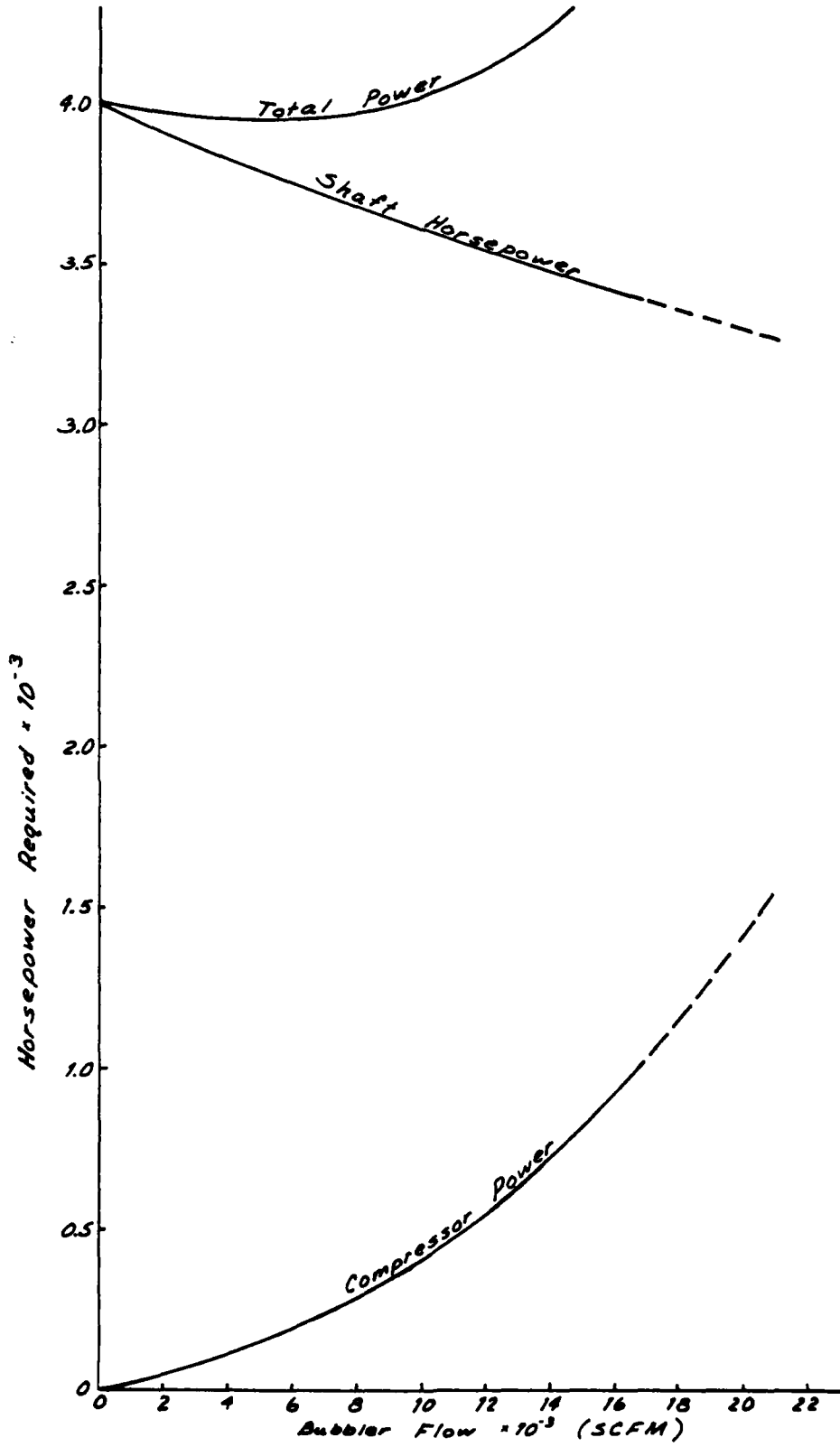


Figure 4.6 : Bubbler Performance at 5 Knots in 1.5 ft of 125.5 psi Solid Ice

Where:

- R = resistance to movement
- ρ_i = mass density of ice
- g = gravitational constant
- B = beam at the waterline
- h = ice or brash thickness
- v = velocity of the ship

The data for each separate flow rate was submitted to a forced regression fit and the results of this are tabulated in Table 4.3. As in Table 4.2, the first five columns correspond to the settings employed during the test program, the volume flow rate in standard cubic feet per minute at full-scale for these conditions, the compressor power at full-scale for these conditions, the mean value of the dimensionless brash resistance and the mean value of the square of dimensionless velocity. The two coefficients obtained through regression analysis of this data follow with the last column containing the number of points used to determine these coefficients. The same general process employed in analyzing the continuous motion through solid ice was again used to determine predictor for continuous motion through brash ice. First, a plot was made of the slopes for each of the equations as computed. It is very difficult to see where a line should be drawn through these points, therefore, the first three points and last four points are each averaged and plotted as triangles on Figure 4.7. A line drawn through these two mean points is used to develop a family of curves having changing slope and also fitting the mean of all the data. These new slopes were employed as shown in Table 4.4 to calculate a new intercept value for these conditions. The C_4 and C_5 estimated values represent a smooth family of curves which can be used to predict the performance of the 140-FT. WYTM through brash. One serious problem with the data from the brash tests, is that the data was obtained in 3 ft of ice, well below the maximum capabilities of the WYTM. These predictor equations from Table 4.4 were employed to develop the resistance in 6 ft of brash from data obtained in 3 ft of brash. This has its limitations in that it must be assumed that the extrapolation is correct from 3 ft to 6 ft. On the other hand, it gives us a better idea of the performance of the tug nearer its limiting conditions. The most likely disadvantage of this method is that it may emphasize the effect of the air bubbler system as the dimensionless equation is extrapolated to twice the test thickness. The predictor equations are plotted on

TABLE 4.3 REGRESSION OF BRASH RESISTANCE DATA

Name	Vol. ft ³ /m	Compressor Power HP	$\frac{R}{\rho_i g B h^2}$ mean	$\left(\frac{v}{\sqrt{gh}}\right)^2$ mean	C ₄	C ₅	# of Points
Q ₀	0	0	.551	.273	.568	-.0620	10
Q _{4B}	1,000	28	.606	.280	.475	.467	7
Q _{3A}	2,000	57	.590	.321	.595	-.0144	7
Q ₁	4,000	118	.692	.266	.504	.710	9
Q ₂	8,000	283	.610	.217	.564	.214	6
Q ₃	12,250	567	.483	.273	.277	.753	4
Q ₄	16,800	1,020	.380	.163	.384	-.0234	<u>4</u>
							47

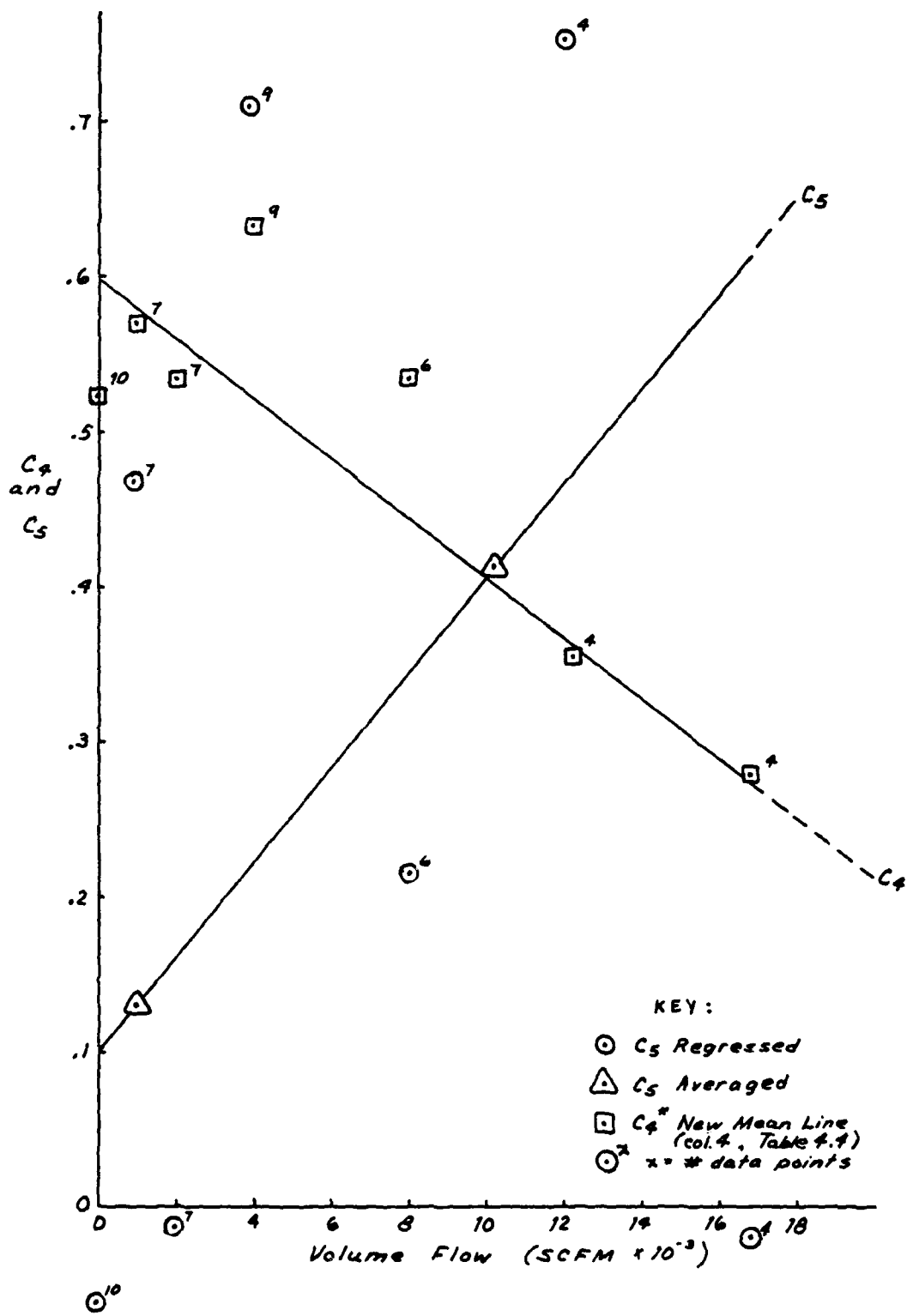


Figure 4.7: Brash Ice Predictor

TABLE 4.4 BRASH PREDICTOR EQUATION

Name	Vol.	C_5 estimated	C_4^*	C_4 estimated
Q_0	0	0.100	0.524	0.600
Q_{4B}	1,000	0.130^1	0.570	0.582
Q_{3A}	2,000	0.162	0.534	0.562
Q_1	4,000	0.222	0.633	0.522
Q_2	8,000	0.345	0.535	0.444
	10,125	0.413^2		
Q_3	12,250	0.476	0.353	0.362
Q_4	16,800	0.616	0.279	0.275

$$*C_4 = \left(\frac{R}{\rho_i g B h^2} \right)_{\text{mean}} - (C_5)_{\text{estimated}} \times \left(\frac{v^2}{gh} \right)_{\text{mean}}$$

$$^1 \frac{(C_5)_{Q_0} + (C_5)_{Q_{4B}} + (C_5)_{Q_{3A}}}{3}$$

$$^2 \frac{(C_5)_{Q_1} + (C_5)_{Q_2} + (C_5)_{Q_3} + (C_5)_{Q_4}}{4}$$

both the dimensionless basis and the six feet of brash ice in Figure 4.8. The ship performance curves, of course, only apply to the dimensional axes. Intersections of the resistance curves and the thrust curves are operating points at which the tug will proceed in a continuous fashion through 6 ft of brash. This figure was used to evaluate the performance of the bubbler system at 1, 3 and 5 knots through 6 ft of brash ice. This information is then plotted in Figures 4.9 through 4.11. The plots were made in the same fashion as those for the uniform sheet ice and again the optimum operating condition is the minimum total power point as shown on these curves. One thing that we do see in the brash ice is that there are occasions when more air flow is required than the presently installed compressor can provide.

4.4 Starting Performance

In addition to the towed resistance tests, a series of starting resistance tests were performed in both solid and brash ice. This was the first time that tests of this sort have been performed at ARCTEC and a number of initial problems were encountered. The time required to get the towing apparatus started allowed creep to take place in the ice sheet and very low values of resistance were obtained during the first two days of the tests. On the last two days, however, the procedure was refined such that the ship was forced by hand into the ice sheet and quickly attached to the towing apparatus for the very slow speed starting force determination. Very consistent results were obtained. The best of these results are plotted in Figure 4.12. Starting resistance is plotted as a function of the bubbler flow for three particular ice conditions in which tests were actually conducted. Also plotted on this figure, as dotted lines, are the propeller thrust of the installed propulsion system. Using the propeller thrust curves, the necessary shaft horsepower to start the tug moving was then calculated and plotted in Figure 4.13. When this shaft horsepower is added to the compressor power, a total power curve is produced which is similar to those produced for continuous motion in solid ice and brash earlier. For the starting resistance, it appears that a much lower bubbler flow is necessary to achieve optimum results. A flow of approximately 4,000 scfm in 3.6 feet of brash gives the best performance. Only slightly higher flows are required for the two sheet ice tests which were performed. There should be caution applied to these performance curves in that the ice was a great deal weaker than the target value of 126.5 psi. The lower curve in fact, corresponds more to melting sea ice whereas the upper curve is intermediate between sea ice and fresh

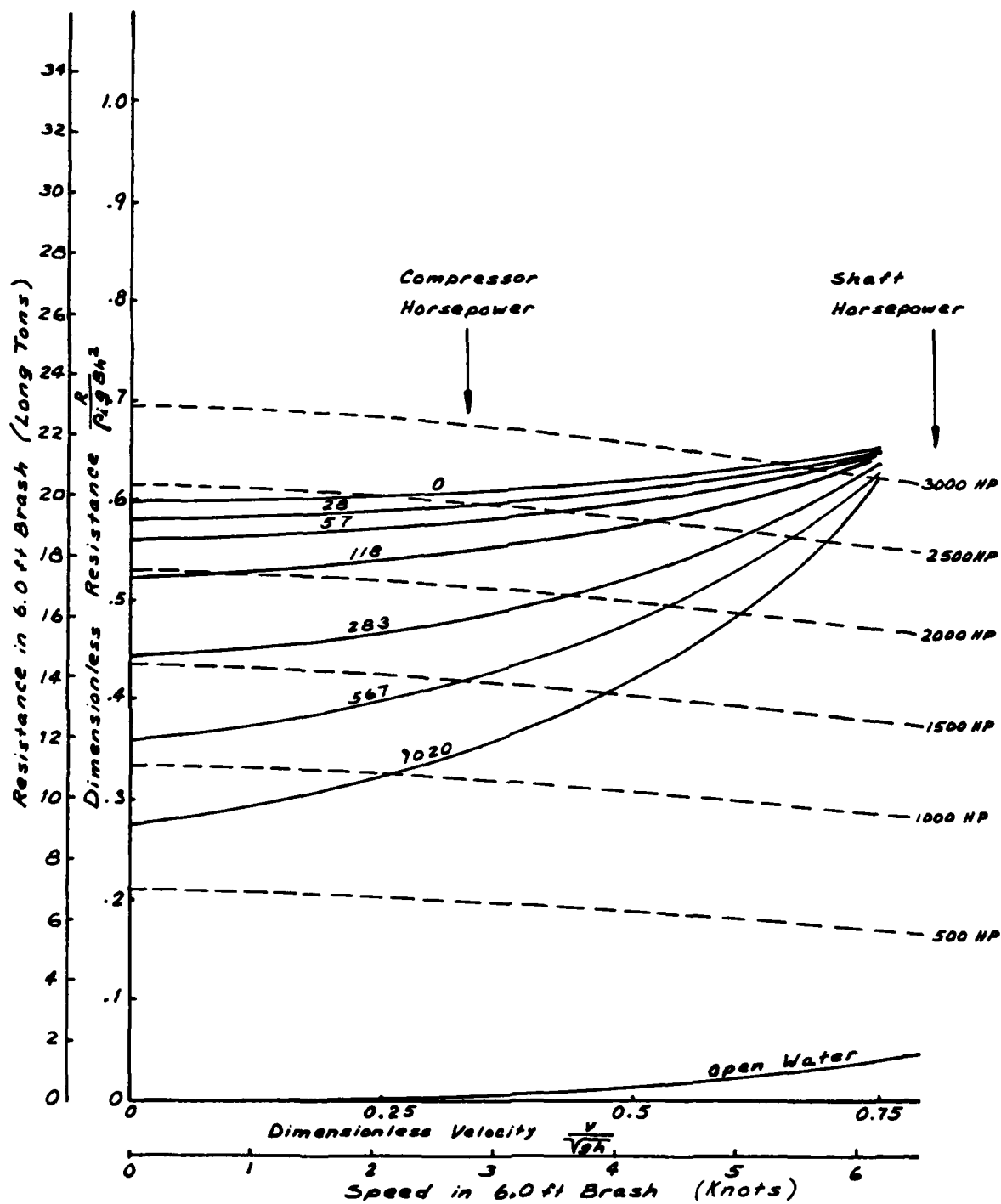


Figure 4.8: Tug with Bubbler in 6.0 ft Brash

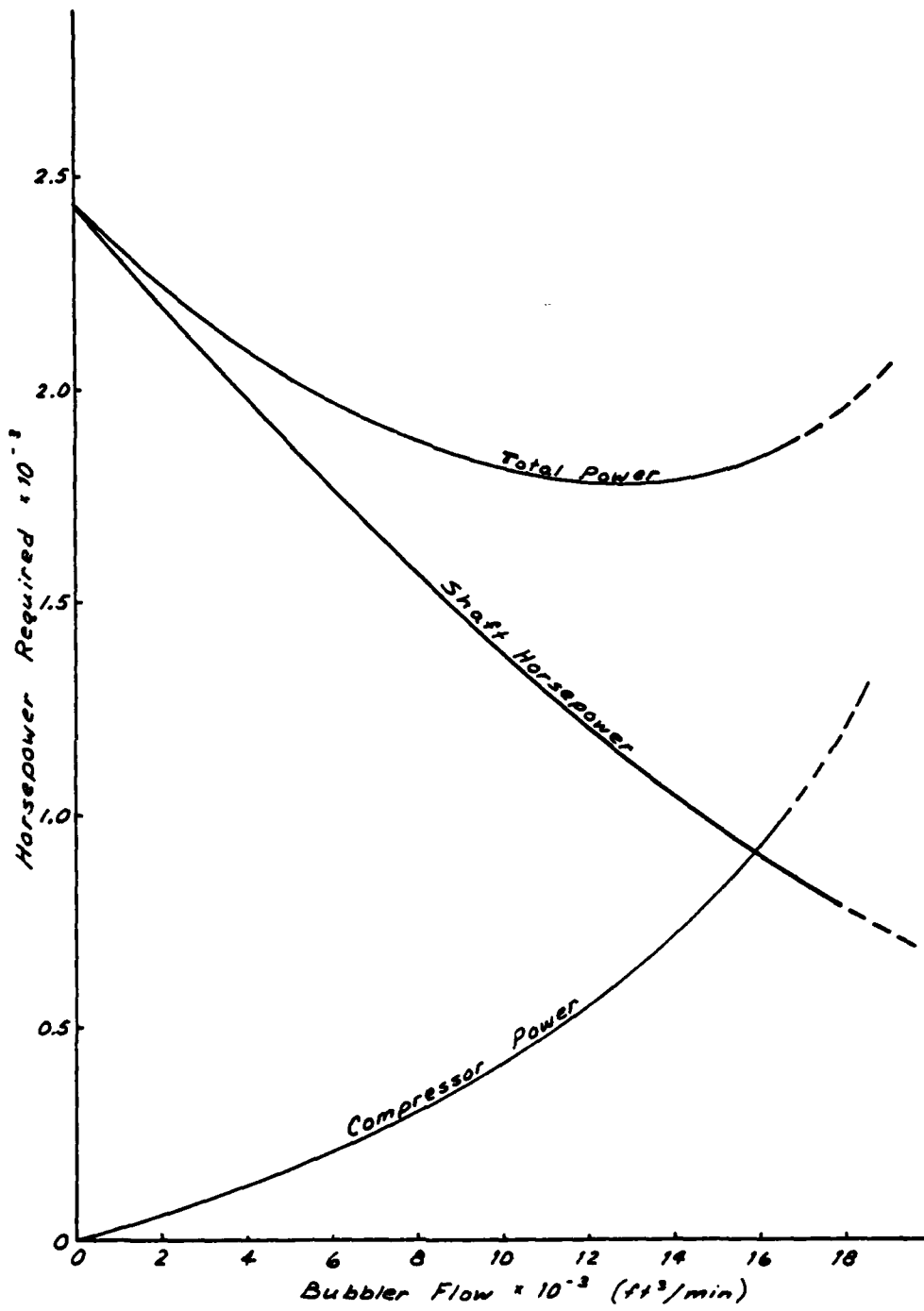


Figure 4.9: Bubbler Performance at 1 Knot in 6.0 ft Brush

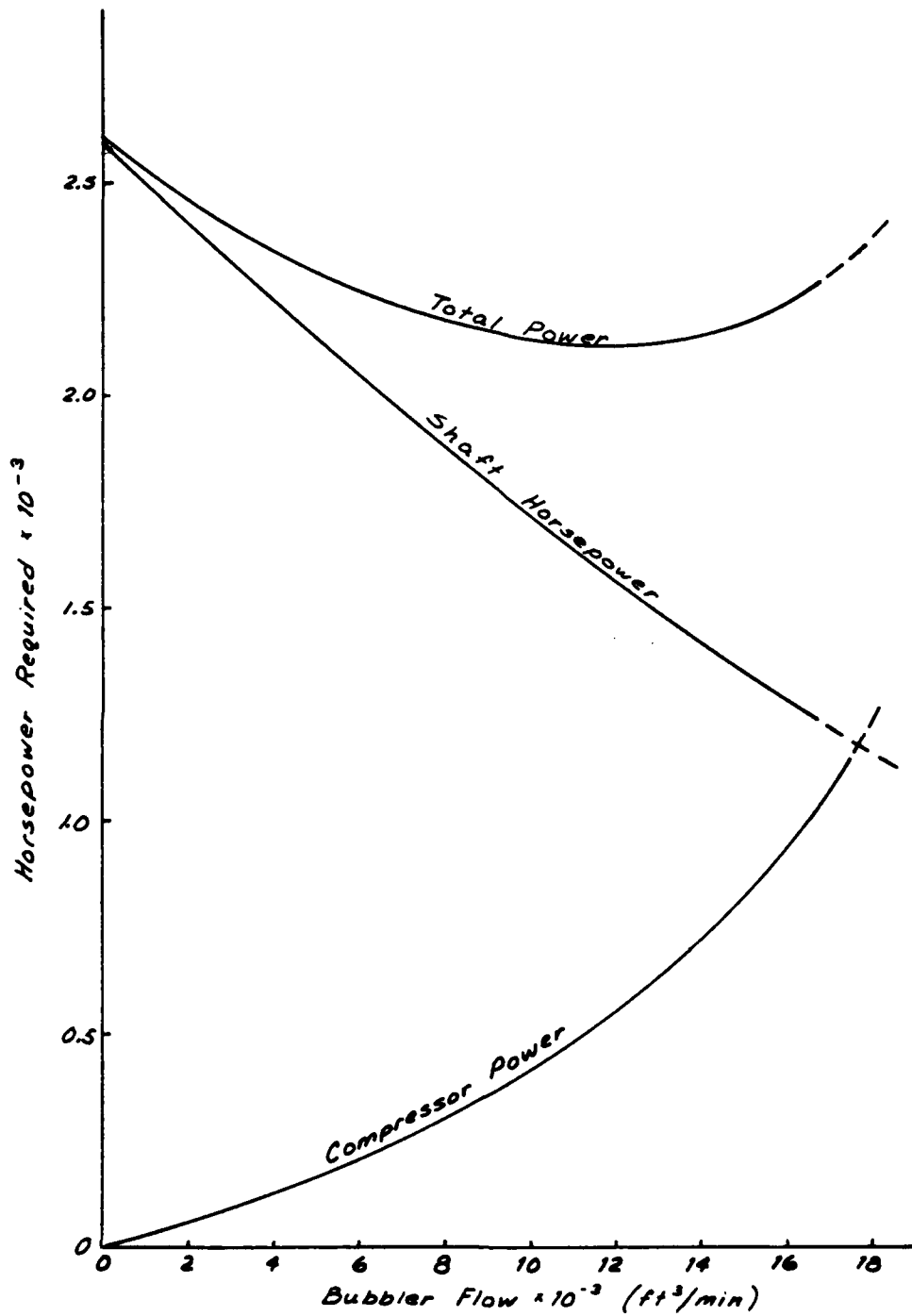


Figure 4.10 : Bubbler Performance at 3 Knots in 6.0 ft Brash

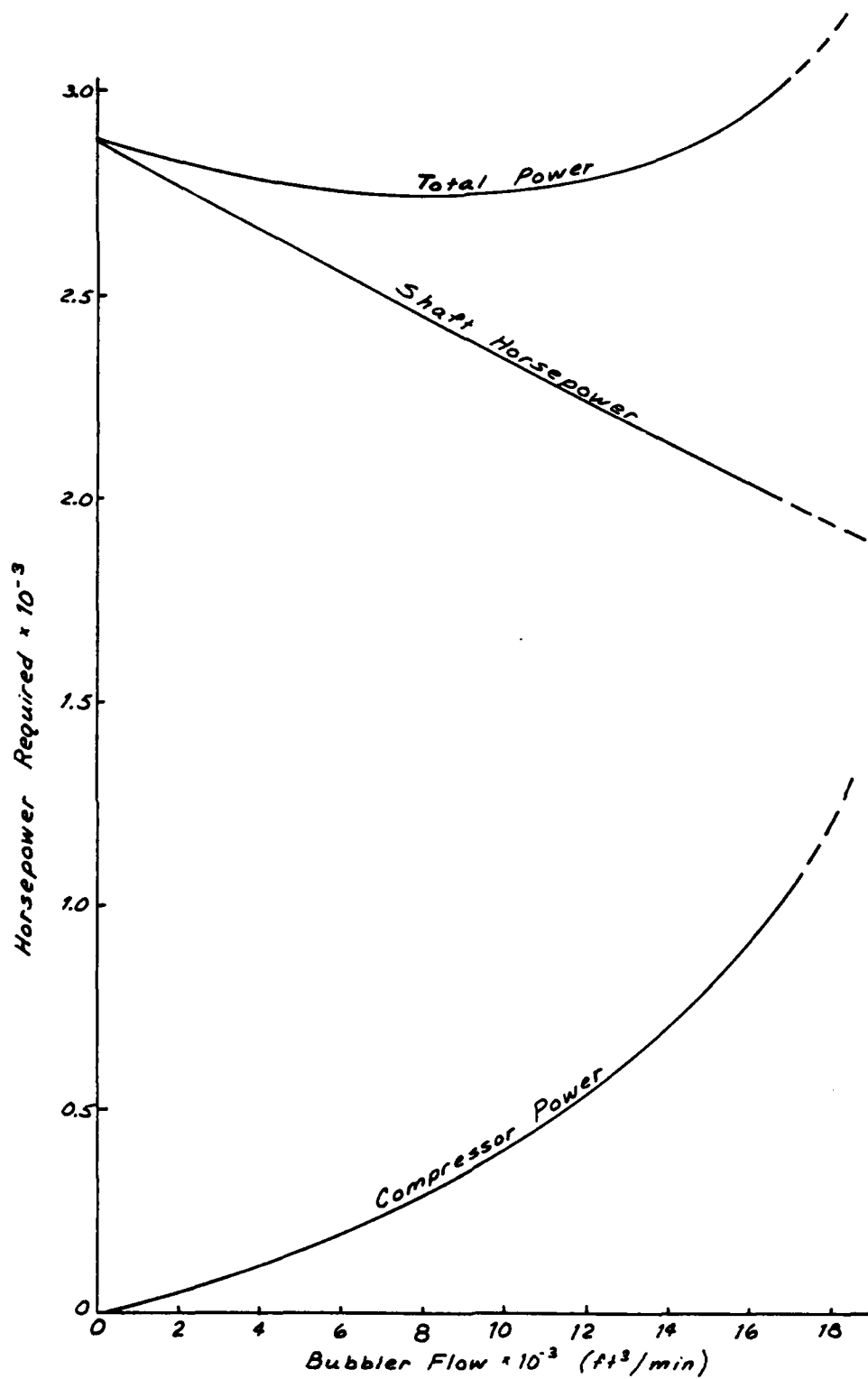


Figure 4.11: Bubbler Performance at 5 Knots in 6.0 ft Brash

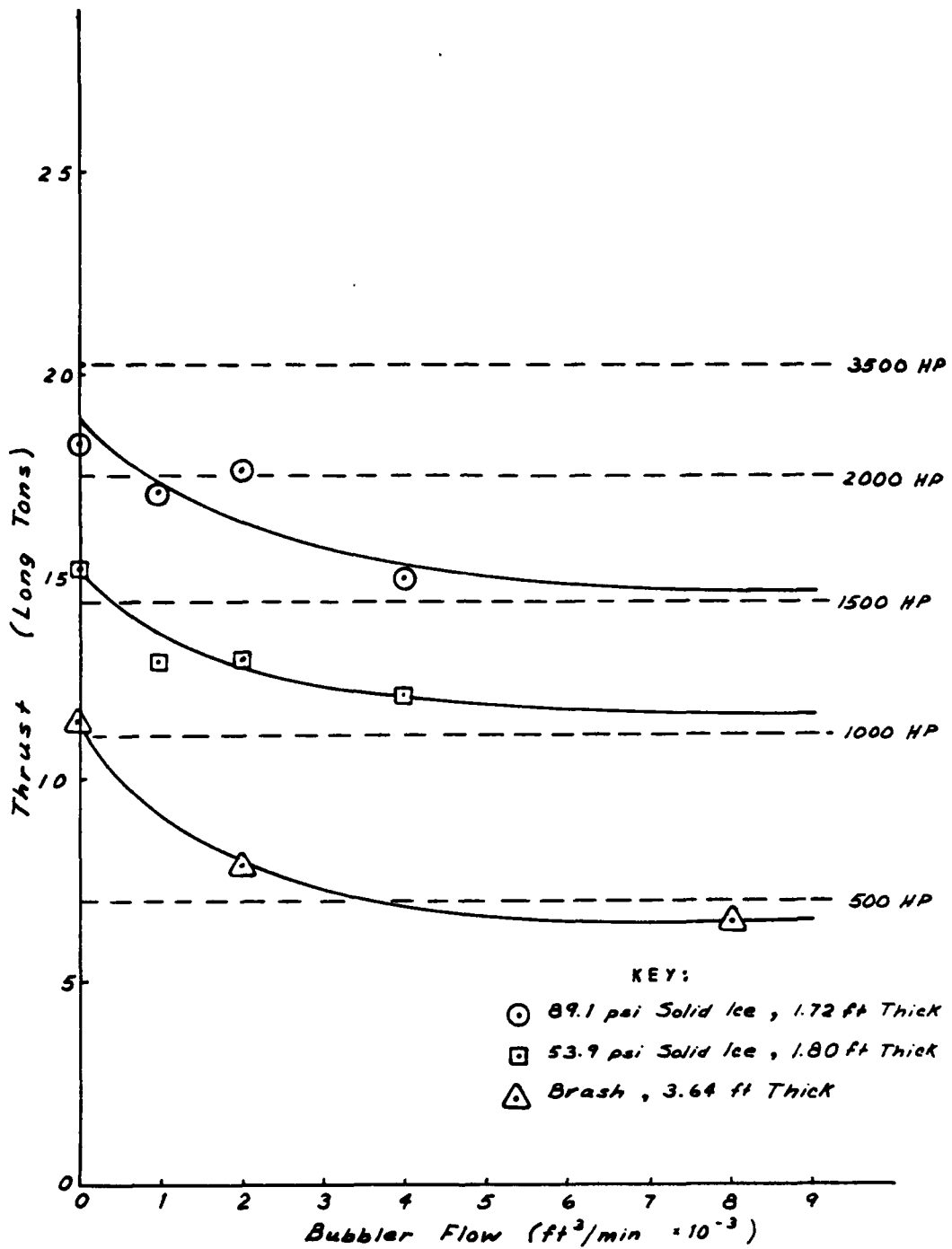


Figure 4.12: Starting Resistance

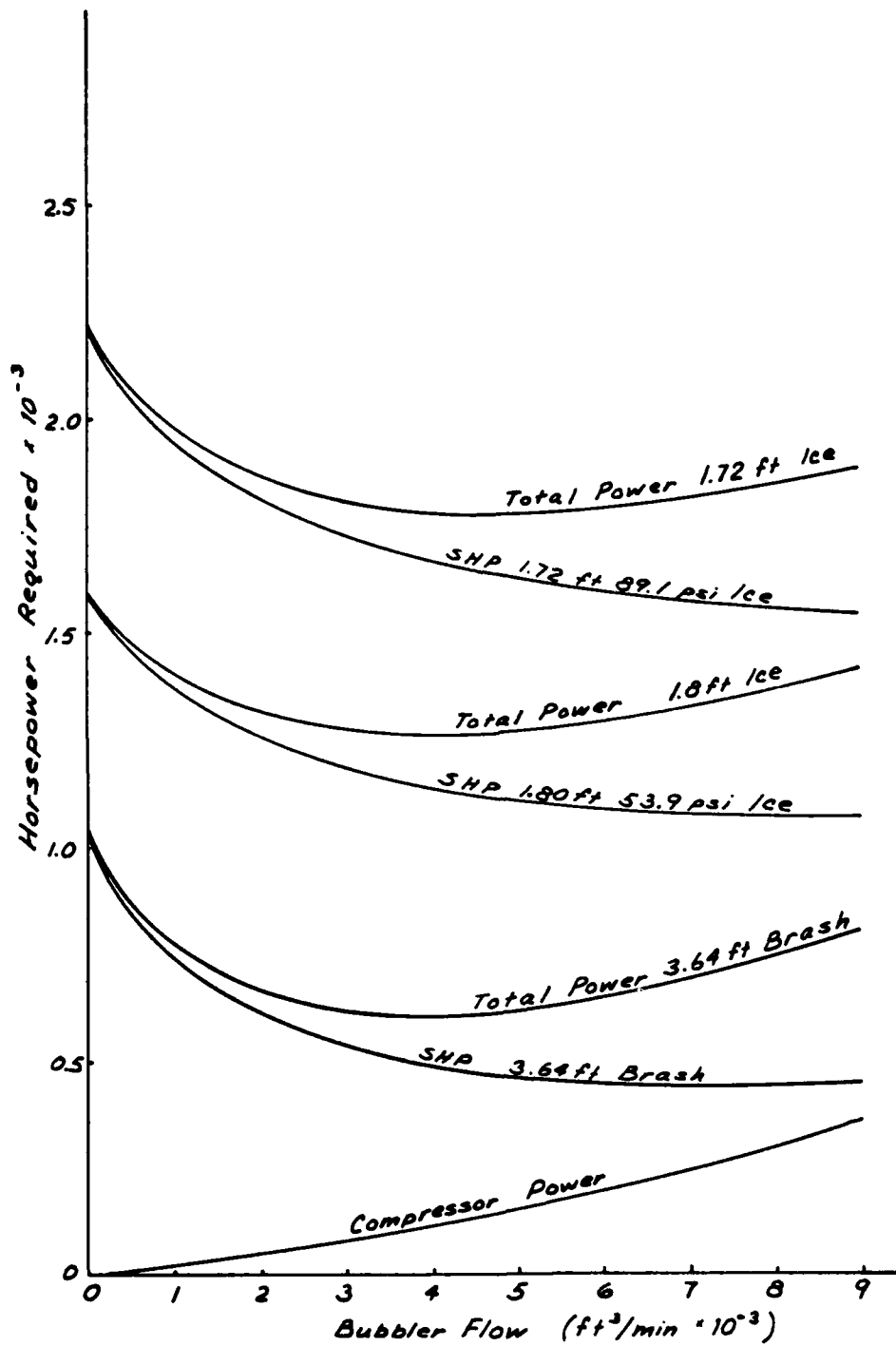


Figure 4.13: Starting Performance

water ice. The data points from these three curves is plotted on a dimensionless basis in Figure 4.14. This shows the actual percentage reduction in starting resistance due to the installation of an air bubbler system. This also clearly shows that the design flow is sufficient to produce nearly minimal starting resistance.

4.5 Analysis of the Photographic Data

The underwater movies which were taken clearly show the change in performance of the air bubbler system with speed and flow rate. The nozzles on the bow manifold do not discharge downward so that seachests located aft of the bow manifold would not appear to be subject to injection of air. The movies also clearly show that the train of bubbles from the nozzles rising at a constant speed is swept further and further aft as the speed of the tug increases. Therefore, the section of the bow subjected to the heaviest amount of breaking is never covered with air and the bow shoulders are covered with air less as speed increases. There is a great deal more film available for the condition of operation in sheet ice than there is available to study operation of the bubbler system in brash. In sheet ice the bubbles are trapped between the surface of the ice and the hull and seem to effectively keep the ice away from the hull. In brash, because of the broken coating, there appears to be some leakage of the air out from the side of the ship and the uneven surface requires more air. If possible, the technical film to examine how the bubbles travel along the hull should be viewed.

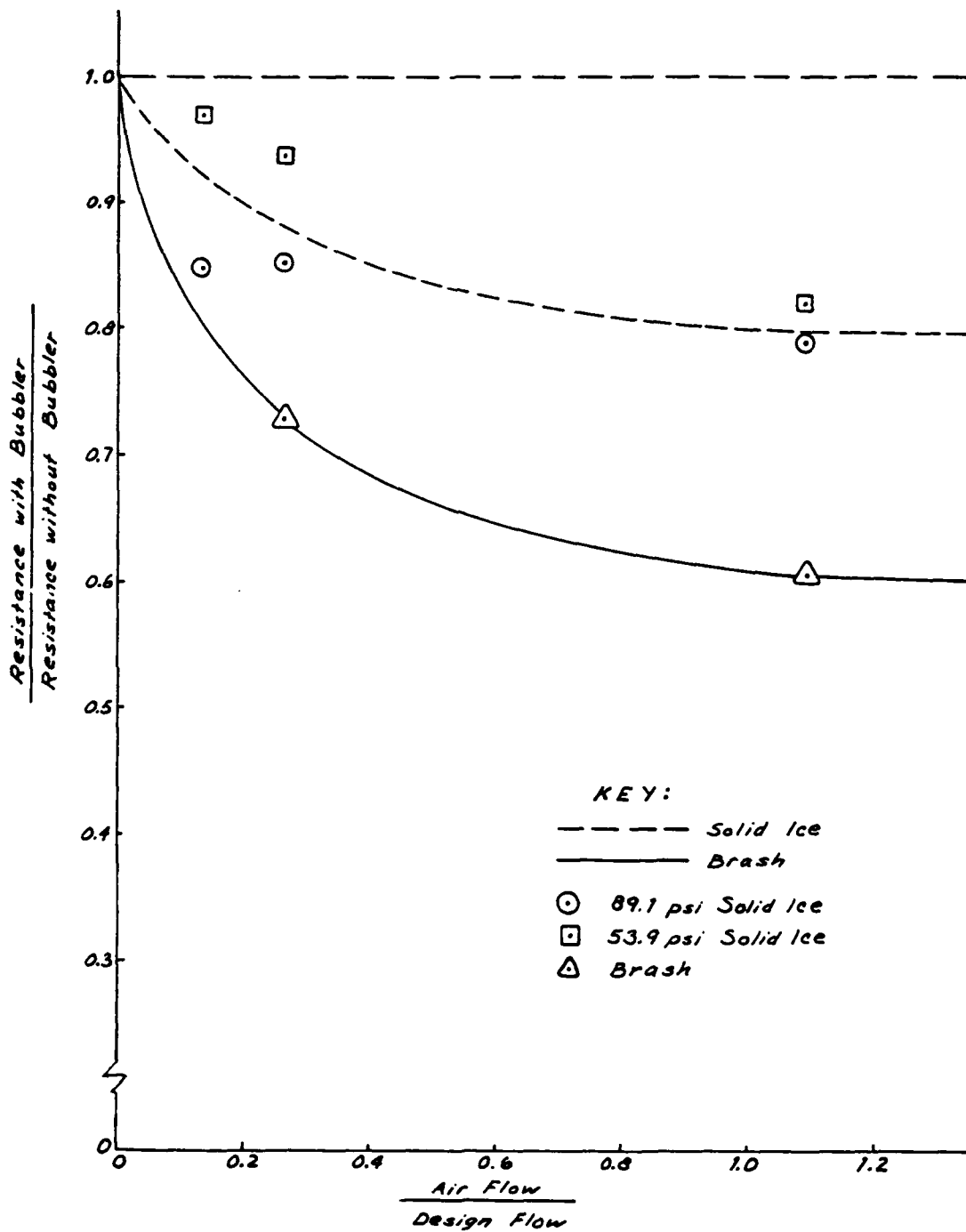


Figure 4.14 : Dimensionless Starting Resistance

5. CONCLUSIONS AND RECOMMENDATIONS

5.1 Conclusions

1. The bubbler system as designed at 7,500 scfm is effective in reducing the resistance of the icebreaking tug and also in reducing its fuel consumption. As can be seen in the performance curves plotted in section 4, in every case the total horsepower required to proceed through a given ice condition was reduced due to use of the air bubbler system. The system is most effective at low velocities and in brash ice. For starting resistance in brash ice, the resistance will only be 60% of that without a bubbler system when the bubbler system is operated at its designed conditions. For starting conditions in solid ice, the resistance is reduced by 20% with operation of a bubbler system at its designed conditions.
2. A good distribution of the air coating is obtained along the shoulders and side of the tug by the air bubble train. There appears to be no need to place intermediate nozzles in order to get a satisfactory distribution of air.
3. Most of the bow is not covered by air bubbles. In future designs more effort needs to be given to the possibility of locating air nozzles further forward. As was shown in the coating tests completed prior to this program, the area immediately adjacent to the stem is that contributing the most to icebreaking resistance. It therefore seems logical that to be most effective an air bubbler system should coat this particular area.

5.2 Recommendations

1. As soon as the full-scale WYTM becomes available in its initial encounter with ice, a series of full-scale tests should be conducted to obtain at least a few data points which could be used to compare with these model scale results. This would then improve the confidence in the effects of various flow rates on performance as was determined in this series.

2. The use of additional nozzles forward of those used in this program should be examined, particularly in future designs. It would be possible to equip the model of the 140 FT. WYTM tug with additional nozzles further forward to study this particular possibility before any further design work is accomplished.
3. A study should be conducted of the trade-off between employment of a air bubbler system and application of a low friction underwater coating. It is known now that both of these systems will improve the performance of icebreaking ships but the interaction between the two is still not known. For example, we do not know if the bubbler system mechanism for reducing icebreaking resistance is the same as that of the low friction coating: in that forming a film of air and water between the ice and the hull it reduces hull/ice friction. This question might be answered by coating the 140 FT. WYTM with a smooth paint surface and repeating a few tests with the bubbler to see if the benefits are still obtained with the smooth hull.

6. REFERENCES

1. Lecourt, E.J., "Icebreaking Model Tests of the 140-FOOT WYTM," ARCTEC Report 202C-2, Contract DOT-CG-50383-A, September 1975.
2. Lecourt, E.J., "Air Bubbler System Design for the 140-FOOT WYTM," ARCTEC Report 202C-3, Contract DOT-CG-50383-A, January 1976.
3. ARCTEC, Incorporated "Test Plan for Model Tests in Ice to Confirm Effectiveness of the 140-FOOT WYTM Air Bubbler System," ARCTEC Report 354C-1, Contract DOT-CG-64,242-A, December 1976.
4. ARCTEC, Incorporated "Proposal-Study to Conduct Model Testing in Ice to Confirm Effectiveness of 140-FOOT WYTM Air Bubbler System," Solicitation CG-64-242A, August 1976.
5. Remmers, K.D. and R. Hecker, "Powering Predictions for the United States Coast Guard 140-FOOT WYTM [Icebreaking Tugboat] (Model 5336-Propeller 4657)" NSRDC Report SPD-223-18, July 1975.
6. Baumeister, Theodore, editor, Mark's Mechanical Engineer's Handbook, Sixth Edition, McGraw Hill, New York, 1958, Chapter 14.
7. Lewis, J.W., "Ship Model Ice Resistance Experiments," Technical Report 0029, Contract No. DOT-CG-13189-A, ARCTEC, Incorporated, October, 1972.
8. Kobus, Helmut E., "Analysis of the Flow Induced by Air Bubbler Systems," ASCE, Proceedings of the Eleventh Conference on Coastal Engineering, London, England, September, 1968.

APPENDIX A
RESISTANCE DATA

TABLE A.1 Model Data

Solid Ice
Brash
Starting

TABLE A.2 Dimensionless Data

Solid Ice
Brash

TABLE A.3 Data in Full-Scale Units

Solid Ice
Brash
Starting

SHEET ICE

TABLE A-1. MODEL DATA

#	Name	Time	R N	h mm	v mm/sec	σ_f kPa	p_1 kPa	p_2 kPa	p_3 kPa	p_4 kPa	T_1 °C	T_2 °C	T_3 °C	T_4 °C	Q_T m ³ /h	P_T watts
1	Q ₀	1025	19.1	19.0	89	55.6	--	--	--	--	--	--	--	--	--	--
2	↓	--	25.7	19.4	281	↓	--	--	--	--	--	--	--	--	--	--
3	↓	1031	28.0	18.3	494	↓	--	--	--	--	--	--	--	--	--	--
4	Q ₄	--	10.9	19.4	73	12.45+	12.45+	--	--	--	2	2	0	0	10.22	11.44
5	↓	--	21.7	19.7	281	"	"	"	"	"	"	"	"	"	"	"
6	↓	1049	24.9	18.9	487	"	"	"	"	"	"	"	"	"	"	"
7	Q ₁	1543	16.1	18.8	306	32.5	2.86	3.23	3.48	2.74	4	10	0	5	2.38	1.30
8	↓	--	21.8	17.8	498	↓	"	"	"	"	10	6	0	3	"	"
9	Q ₂	1556	9.63	20.0	76	↓	4.73	3.98	6.48	5.48	9	5	0	3	4.81	3.12
10	↓	--	24.1	18.1	487	↓	"	"	"	"	6	3	0	2	"	"
11	Q ₃	1609	9.77	18.9	74	↓	8.72	5.48	12.45	9.46	8	3	0	2	7.37	6.25
12	↓	--	16.6	19.1	279	↓	"	"	"	"	5	1	0	1	"	"
13	Q ₁	--	15.7	20.4	78	49.2	3.23	1.86	3.23	3.11	-1	-1	-1	-1	2.39	1.310
14	↓	0927	20.0	21.1	274	↓	"	"	"	"	"	"	"	"	"	"
15	↓	--	28.0	21.9	478	↓	"	"	"	"	"	"	"	"	"	"
16	Q ₀	0931	15.8	20.8	73	↓	--	--	--	--	--	--	--	--	--	--
17	↓	--	16.3	20.1	307	↓	"	"	"	"	"	"	"	"	"	"
18	↓	--	26.1	21.4	489	↓	"	"	"	"	"	"	"	"	"	"
19	Q ₃	1255	13.5	19.5	318	28.4	6.97	2.49	10.96	11.96	0	0	0	0	7.37	6.245
20	↓	1256	22.2	20.1	478	↓	"	"	"	"	0	0	0	0	"	"
21	Q ₄	--	8.4	21.9	76	↓	8.47	3.99	12.45+	12.45+	0	0	0	1	10.03	11.048
22	↓	1303	20.4	19.8	507	↓	"	"	"	"	0	0	0	2	"	"
23	Q ₂	1309	7.7	20.1	75	↓	4.23	2.49	8.71	6.47	0	1	0	2	4.85	3.183
24	↓	1311	16.2	21.0	287	↓	"	"	"	"	"	"	"	"	"	"
25	Q _{4B}	1110	22.5	22.7	303	18.7	1.62	.75	1.99	1.74	7	8	0	8	.59	.2974
26	↓	1112	27.6	22.9	478	↓	"	"	"	"	"	"	"	"	"	"
27	Q ₁	1116	16.8	22.9	76	↓	2.24	1.49	2.24	2.36	10	8	0	6	2.36	1.288
28	↓	1118	24.2	22.5	478	↓	"	"	"	"	"	"	"	"	"	"
29	Q ₂	1123	9.6	22.9	73	↓	2.99	1.24	4.48	7.47	10	7	1	5	4.78	3.127
30	↓	1125	18.3	23.0	273	↓	"	"	"	"	"	"	"	"	"	"

+ Off Scale, estimated 18.7 kPa.

TABLE A-1. (Continued)

SHEET ICE #	Name	Time	R N	h mm	v mm/sec	σ_f kPa	p_1 kPa	p_2 kPa	p_3 kPa	p_4 kPa	T_1 °C	T_2 °C	T_3 °C	T_4 °C	Q_T m ³ /h	P_T watts
31	Q _{3A}	1300	12.3	22.6	80	15.5	1.49	1.24	1.24	1.99	3	1	0	0	1.19	.6278
32	↓	--	16.3	21.9	287	↓	"	"	"	"	"	"	"	"	"	"
33	Q ₀	1316	23.1	23.4	478	↓	"	"	"	"	"	"	"	"	"	"
34	↓	1320	11.2	22.5	76	↓	--	--	--	--	--	--	--	--	--	--
35	↓	--	19.5	22.5	273	↓	--	--	--	--	--	--	--	--	--	--
36	↓	--	23.0	22.7	478	↓	--	--	--	--	--	--	--	--	--	--
37	Q ₂	0830	23.5	19.6	287	30.3	2.49	1.24	5.72	12.45+	3	1	-2	1	4.89	3.216
38	↓	0835	28.5	20.8	537	↓	"	"	"	"	"	"	"	"	"	"
39	Q _{3A}	0840	19.5	21.4	76	↓	1.86	.99	.47	.97	1	0	-1	-1	1.19	.6278
40	↓	0841	27.5	20.9	478	↓	"	"	"	"	"	"	"	"	"	"
41	Q ₁	0945	12.8	21.4	74	↓	1.86	1.12	3.73	12.45+	0	0	-1	0	2.44	1.343
42	↓	0945	23.5	21.4	287	↓	"	"	"	"	"	"	"	"	"	"
43	Q _{4B}	1042	17.7	21.1	80	↓	1.74	1.62	1.49	12.45+	2	13	-1	0	.61	.3194
44	↓	--	19.7	20.4	273	↓	"	"	"	"	"	"	"	"	"	"
45	↓	1044	26.9	22.2	537	↓	"	"	"	"	"	"	"	"	"	"
46	↓	--	17.8	22.1	80	↓	--	--	--	--	--	--	--	--	--	--
47	↓	--	23.0	22.2	273	↓	--	--	--	--	--	--	--	--	--	--
48	↓	--	27.8	21.9	478	↓	--	--	--	--	--	--	--	--	--	--

TABLE A-1. (Continued)

BRASH ICE #	Name	Time	R N	h mm	v mm/sec	σ_f kPa	p_1 kPa	p_2 kPa	p_3 kPa	p_4 kPa	T_1 °C	T_2 °C	T_2 °C	T_2 °C	Q_T m ³ /h	P_T watts
1	Q ₁	1807	3.94	46.7	308	--	3.99	2.74	3.49	2.74	-2	-1	0	-1	2.40	1.321
2	Q ₂	--	5.32	38.4	493	--	"	"	"	"	"	"	"	"	"	"
3	Q ₃	1812	2.66	48.3	86	--	2.72	4.98	12.45+	9.71	2	0	0	0	7.44	6.377
4	Q ₄	--	5.65	53.3	418	--	"	"	"	"	"	"	"	"	"	"
5	Q ₄	1830	5.25	50.6	76	--	7.47	12.45+	12.45+	"	3	0	0	0	10.15	11.257
6	Q ₁	--	4.03	47.3	279	--	"	"	"	"	"	"	"	"	"	"
7	Q ₁	1710	5.23	49.4	81.5	--	1.87	1.87	2.74	5.98	0	0	0	0	2.39	.8977
8	Q ₁	--	5.71	45.8	287	--	"	"	"	"	"	"	"	"	"	"
9	Q ₁	1715	7.29	41.7	461	--	"	"	"	"	"	"	"	"	"	"
10	Q ₀	1718	4.21	43.1	111	--	--	--	--	--	--	--	--	--	--	--
11	Q ₁	--	3.96	49.2	318	--	--	--	--	--	--	--	--	--	--	--
12	Q ₁	1719	7.31	55.6	478	--	--	--	--	--	--	--	--	--	--	--
13	Q ₃	1758	3.86	46.3	287	--	2.62	2.24	7.22	11.33	1	3	1	2	7.28	6.069
14	Q ₄	--	4.99	41.7	478	--	"	"	"	"	"	"	"	"	"	"
15	Q ₄	--	1.77	46.3	83	--	6.10	3.99	12.45+	"	0	0	1	1	9.99	11.004
16	Q ₄	--	3.59	50.8	478	--	"	"	"	"	"	"	"	"	"	"
17	Q ₂	1823	2.15	39.4	287	--	3.73	2.49	5.48	6.48	0	1	0	1	4.83	3.161
18	Q ₄	--	3.54	42.5	318	--	"	"	"	"	"	"	"	"	"	"
19	Q ₄	1815	5.40	45.8	299	--	1.86	2.74	2.12	1.12	4	12	2	7	.59	.297
20	Q ₄	--	6.70	43.1	537	--	"	"	"	"	"	"	"	"	"	"
21	Q ₁	1818	5.14	40.8	102	--	1.74	2.98	2.49	2.37	4	12	2	6	2.36	1.299
22	Q ₁	1819	7.37	43.8	478	--	"	"	"	"	"	"	"	"	"	"
23	Q ₂	1821	6.78	41.9	83	--	2.73	3.48	5.23	4.73	5	12	3	6	4.77	3.073
24	Q ₂	--	4.28	41.3	292	--	"	"	"	"	"	"	"	"	"	"
25	Q ₃ A	1950	3.81	47.5	86	--	2.12	2.74	3.36	1.74	1	1	3	3	1.19	.6278
26	Q ₃ A	--	4.22	47.5	307	--	"	"	"	"	"	"	"	"	"	"
27	Q ₀	--	5.45	50.0	478	--	"	"	"	"	"	"	"	"	"	"
28	Q ₀	1955	6.33	50.0	83	--	--	--	--	--	--	--	--	--	--	--
29	Q ₀	--	5.80	48.3	279	--	--	--	--	--	--	--	--	--	--	--
30	Q ₀	--	5.32	42.5	478	--	--	--	--	--	--	--	--	--	--	--

TABLE A-1. (Continued)

BRASH ICE		Time	R N	h mm	v mm/sec	σ_f kPa	p ₁ kPa	p ₂ kPa	p ₃ kPa	p ₄ kPa	T ₁ °C	T ₂ °C	T ₃ °C	T ₄ °C	Q _T m ³ /h	P _T watts
#	Name															
31	Q ₂	1554	2.8	38.7	287	--	2.49	3.11	11.21	5.35	1	2	0	2	4.85	3.183
32	Q _{3A}	--	4.9	39.4	478	--	"	"	"	"	"	"	"	"	"	"
33	Q _{3A}	--	4.5	36.9	159	--	2.24	1.49	2.24	2.24	0	1	0	1	1.19	.6278
34	Q ₁	--	5.48	38.1	478	--	"	"	"	"	"	"	"	"	"	"
35	Q ₁	--	4.0	41.9	159	--	2.12	1.99	2.74	3.24	0	1	0	1	2.39	1.310
36	Q _{4B}	1611	2.5	43.3	292	--	"	"	"	"	"	"	"	"	"	"
37	Q _{4B}	1650	4.2	38.7	174	--	1.74	1.74	1.99	1.87	0	0	0	0	.59	.3084
38	Q ₀	--	3.5	38.7	279	--	"	"	"	"	"	"	"	"	"	"
39	Q ₀	--	4.2	40.0	478	--	"	"	"	"	"	"	"	"	"	"
40	Q ₀	1700	4.2	41.9	152	--	--	--	--	--	--	--	--	--	--	--
41	Q ₀	--	2.9	38.3	299	--	--	--	--	--	--	--	--	--	--	--
42	Q _{3A}	1703	3.6	43.3	478	--	--	--	--	--	--	--	--	--	--	--
43	Q _{3A}	1745	3.7	45.8	299	--	1.74	1.49	1.86	2.37	0	0	0	0	1.19	.6278
44	Q _{4B}	--	3.6	40.8	522	--	"	"	"	"	"	"	"	"	"	"
45	Q _{4B}	1748	3.7	45.6	84	--	1.49	1.49	1.74	2.12	0	0	0	0	.59	.3084
46	Q ₀ *	--	3.0	47.5	304	--	"	"	"	"	"	"	"	"	"	"
47	Q ₀ *	--	1.6	46.7	318	--	--	--	--	--	--	--	--	--	--	--
48	Q ₀ *	1753	3.3	45.0	478	--	--	--	--	--	--	--	--	--	--	--

* Deleted from regression analysis due to wide fluctuation in load.

TABLE A-1 (Continued)

STARTING RESISTANCE

#	Name	Ice		R N	h mm	v mm/sec	σ_f kPa	p ₁ kPa	p ₂ kPa	p ₃ kPa	p ₄ kPa	T ₁ °C	T ₂ °C	T ₃ °C	T ₄ °C	Q _T m ³ /h	P _T watts
		Condition	h mm														
1	Q ₀	Brash	2.69	35.0	4.19	--	--	--	--	--	--	--	--	--	--	--	--
2	Q ₂	↓	2.65	↓	4.19	--	5.48	7.97	8.72	5.73	--	-2	-1	-1	-1	4.89	3.216
3	Q ₄	↓	4.71	↓	4.19	--	12.45	10.71	12.45+	--	--	0	0	0	0	10.14	11.235
4	Q ₁	Solid	14.75	21.6	4.19	23.4	1.99	1.99	2.86	7.22	--	0	0	0	0	2.40	1.321
5	Q ₁	↓	10.15	↓	4.19	↓	.75	1.74	1.49	6.72	--	0	0	0	0	2.39	1.310
6	Q ₀	↓	8.30	↓	4.15	↓	--	--	--	--	--	--	--	--	--	--	--
7	Q ₀	Solid	10.94	22.9	3.90	15.5	--	--	--	--	--	--	--	--	--	--	--
8	Q _{4B}	↓	9.29	↓	4.15	↓	2.24	1.25	10.21	11.21	--	-1	-1	-1	-1	.61	.3194
9	Q _{3A}	↓	9.34	↓	4.04	↓	1.74	1.12	4.73	3.24	--	-1	0	-1	-1	1.19	.6278
10	Q ₁	↓	8.68	↓	4.04	↓	2.24	1.25	4.48	5.48	--	-1	0	-1	-1	2.40	1.321
11	Q ₀	Solid	13.14	21.9	4.19	25.6	--	--	--	--	--	--	--	--	--	--	--
12	Q _{3A}	↓	12.32	↓	4.04	↓	1.49	1.62	1.25	12.45+	--	0	0	0	0	1.22	.6388
13	Q _{4B}	↓	12.70	↓	4.04	↓	1.62	1.12	1.62	2.74	--	0	0	0	0	.59	.308
14	Q ₁	↓	10.80	↓	4.19	↓	2.12	2.62	2.99	9.96	--	0	0	0	0	2.41	1.321
15	Q _{4B}	Brash	3.80	46.25	3.75	--	1.49	2.74	1.49	1.99	--	0	0	0	0	.59	.3084
16	Q _{3A}	↓	5.70	↓	3.90	↓	"	"	"	"	--	"	"	"	"	1.19	.6278
17	Q ₂	↓	4.74	↓	3.90	↓	2.99	2.12	8.34	12.45+	--	0	0	0	0	4.92	3.238
18	Q ₀	↓	8.18	↓	4.04	↓	--	--	--	--	--	--	--	--	--	--	--
19	Q ₀	↓	4.00	↓	4.04	↓	--	--	--	--	--	--	--	--	--	--	--
20	Q ₀	↓	7.47	↓	4.04	↓	--	--	--	--	--	--	--	--	--	--	--
21	Q ₀	↓	3.17	↓	4.04	↓	--	--	--	--	--	--	--	--	--	--	--

TABLE A-2 DIMENSIONLESS DATA

SHEET ICE

#	Q	$\frac{R}{\rho_w g B h^2}$	$\frac{v}{\sqrt{gh}}$	$\frac{\sigma}{\rho_w g h}$	$\sigma' \times v'$
1	Q ₀	12.4	.206	297	61.3
2	↓	16.0	.644	291	187
3	↓	19.6	1.167	308	360
4	Q ₄	6.78	.167	291	48.7
5	↓	13.1	.639	286	183
6	↓	16.3	1.132	299	338
7	Q ₁	10.7	.713	175	125
8	↓	16.1	1.192	185	221
9	Q ₂	5.63	.172	165	28.3
10	↓	17.2	1.156	182	211
11	Q ₃	6.40	.172	175	30.0
12	↓	10.6	.645	173	111
13	Q ₁	8.83	.174	245	42.7
14	↓	10.51	.602	237	142.6
15	↓	13.66	1.032	228	235.2
16	Q ₀	8.54	.162	240	38.8
17	↓	9.44	.692	248	171.8
18	↓	13.33	1.068	233	249.1
19	Q ₃	8.31	.727	148	107.5
20	↓	12.85	1.077	143	154.4
21	Q ₄	4.10	.164	132	21.6
22	↓	12.17	1.151	146	167.5
23	Q ₂	4.46	.169	143	24.2
24	↓	8.59	.632	137	86.8
25	Q _{4B}	10.21	.642	84	53.7
26	↓	12.31	1.009	83	83.6
27	Q ₁	7.49	.160	83	13.3
28	↓	11.18	1.018	84	85.9
29	Q ₂	4.28	.154	83	12.8
30	↓	8.09	.575	82	47.4
31	Q _{3A}	5.63	.170	70	11.8
32	↓	7.95	.619	72	44.5
33	↓	9.87	.998	67	67.1
34	Q ₀	5.18	.162	70	11.3
35	↓	9.01	.581	70	40.6
36	↓	10.44	1.013	69	70.2
37	Q ₂	14.3	.655	157	103
38	↓	15.4	1.189	148	176
39	Q _{3A}	10.0	.166	144	23.8
40	↓	14.7	1.056	147	155

TABLE A-2 DIMENSIONLESS DATA (Continued)

SHEET ICE

#	Q	$\frac{R}{\rho_w g B h^2}$	$\frac{v}{\sqrt{gh}}$	$\frac{\sigma}{\rho_w g h}$	$\sigma' \times v'$
41	Q_1	6.5	.162	144	23.2
42	↓	12.0	.627	144	90.0
43	Q_{4B}	9.3	.176	123	21.7
44	↓	11.1	.610	127	77.8
45	↓	12.8	1.151	117	135
46	Q_0	8.5	.172	118	20.2
47	↓	10.9	.585	117	68.5
48	↓	13.6	1.032	119	122

$\rho_w = 1005 \text{ Kg/m}^3$

$g = 9.80 \text{ m/sec}^2$

$B = 0.434 \text{ m.}$

TABLE A-2 DIMENSIONLESS DATA (Continued)

BRASH ICE					
#	Q	$\frac{R}{\rho_w g B h^2}$	$\frac{v}{\sqrt{gh}}$	$\frac{R}{\rho_i g B h^2}$	$\frac{v^2}{gh}$
1	Q ₁	.423	.455	.450	.207
2	↓	.844	.803	.898	.645
3	Q ₃	.267	.125	.284	.016
4	↓	.465	.578	.495	.334
5	Q ₄	.480	.108	.511	.012
6	↓	.421	.410	.448	.168
7	Q ₁	.501	.117	.533	.014
8	↓	.637	.428	.678	.183
9	↓	.981	.721	1.044	.520
10	Q ₀	.530	.171	.564	.029
11	↓	.383	.458	.407	.210
12	↓	.553	.647	.588	.419
13	Q ₃	.421	.426	.448	.181
14	↓	.671	.748	.714	.559
15	Q ₄	.193	.123	.205	.015
16	↓	.325	.677	.346	.458
17	Q ₂	.324	.150	.345	.023
18	↓	.459	.493	.488	.243
19	Q _{4B}	.602	.446	.640	.199
20	↓	.844	.826	.898	.682
21	Q ₁	.722	.161	.768	.026
22	↓	.899	.729	.956	.531
23	Q ₂	.903	.129	.961	.017
24	↓	.587	.459	.624	.211
25	Q _{3A}	.395	.126	.420	.016
26	↓	.438	.450	.466	.202
27	↓	.510	.683	.542	.466
28	Q ₀	.592	.119	.630	.014
29	↓	.582	.405	.619	.164
30	↓	.689	.740	.733	.548
31	Q ₂	.437	.466	.465	.217
32	↓	.738	.769	.785	.591
33	Q _{3A}	.773	.264	.822	.070
34	↓	.677	.782	.720	.611
35	Q ₁	.533	.248	.567	.061
36	↓	.312	.448	.332	.201
37	Q _{4B}	.656	.282	.698	.079
38	↓	.547	.453	.582	.205
39	↓	.614	.763	.653	.582
40	Q ₀	.560	.237	.596	.056

TABLE A-2 DIMENSIONLESS DATA (Continued)

BRASH ICE					
#	Q	$\frac{R}{\rho_w g B h^2}$	$\frac{v}{\sqrt{gh}}$	$\frac{R}{\rho_i g B h^2}$	$\frac{v^2}{gh}$
41	↓	.462	.488	.491	.238
42	↓	.449	.734	.478	.139
43	↓ _{3A}	.413	.446	.439	.199
44	↓	.506	.825	.538	.681
45	↓ _{4B}	.416	.126	.442	.016
46	↓	.311	.445	.331	.198
47	↓ _{0*}	.172	.470	.183	.221
48	↓	.381	.720	.405	.518

*Deleted from analysis, see Table A-1.

TABLE A-3 DATA IN FULL-SCALE UNITS

SHEET ICE

#	Name	Time	R Long Tons	h ft.	v knots	σ psi.	Q_T SCFM	P_T HP
1	Q_0	1025	26.505	1.49	.847	193	--	--
2		--	35.664	1.52	2.674		--	--
3		1031	38.856	1.43	4.701		--	--
4	Q_4	--	15.126	1.52	.694		16980	1039
5		--	30.113	1.54	2.574		"	"
6		1049	34.554	1.48	4.634		"	"
7	Q_1	1543	22.342	1.47	2.912	115.8	3949	118
8		--	30.252	1.39	4.739		"	"
9	Q_2	1556	13.364	1.56	.723		7997	283
10		--	33.444	1.41	4.634		"	"
11	Q_3	1609	13.558	1.48	.704		12242	567
12		--	23.036	1.49	2.655		"	"
13	Q_1	--	21.787	1.59	.742	170.7	3986	119
14		0927	27.754	1.65	2.607		"	"
15		--	38.856	1.71	4.549		"	"
16	Q_0	0931	21.926	1.63	.694		--	--
17		--	22.620	1.57	2.921		--	--
18		--	36.219	1.67	4.653		--	--
19	Q_3	1255	18.734	1.52	3.026	98.57	12247	567
20		1256	30.807	1.57	4.549		"	"
21	Q_4	--	11.657	1.71	.723		16654	1003
22		1303	24.477	1.55	4.825		"	"
23	Q_2	1309	10.685	1.57	.713		8051	289
24		1311	22.481	1.64	2.731		"	"
25	$Q_4 B$	1110	31.224	1.78	2.883	64.90	979	27
26		1112	38.301	1.79	4.549		"	"
27	Q_1	1116	23.314	1.79	.723		3919	117
28		1118	33.583	1.76	4.549		"	"
29	Q_2	1123	13.325	1.79	.694		7931	284

SHEET ICE

TABLE A-3 DATA IN FULL-SCALE UNITS (Continued)

#	Name	Time	R Long Tons	h ft.	v knots	σ psi.	Q_T SCFM	P_T HP
30	Q_{3A}	1125	25.395	1.80	2.598	64.90	1974	57
31		1300	17.069	1.77	.761	53.80	"	"
32		--	22.619	1.71	2.731		"	"
33		1316	32.056	1.83	4.549		--	--
34	Q_a	1320	15.542	1.76	.723		--	--
35		--	27.060	1.76	2.598		--	--
36		--	31.917	1.78	4.549		--	--
37	Q_2	0830	32.611	1.53	2.731	105.17	8120	292
38		0835	39.549	1.63	5.110		"	"
39		0840	27.060	1.67	.723		1974	57
40	Q_{3A}	0841	38.162	1.63	4.549		"	"
41		0945	17.763	1.67	.704		4051	122
42	Q_1	0945	32.611	1.67	2.731		"	"
43		1042	24.562	1.65	.761		1006	29
44	Q_{4B}	--	27.338	1.59	2.598		"	"
45		1044	37.329	1.74	5.110		--	--
46	Q_a	--	24.701	1.73	.761		--	--
47		--	31.917	1.74	2.598		--	--
48		--	38.578	1.71	4.549		--	--

TABLE A-3 DATA IN FULL-SCALE UNITS

BRASH ICE #	Name	Time	R Long Tons	h ft.	v knots	Q _T SCFM	P _T HP
1	Q ₁	1807	7.384	3.01	4.69	3994	120
2	Q ₃	--	5.468	3.66	2.93	"	"
3	Q ₄	1812	3.692	3.78	.81	12357	579
4	Q ₄	--	7.842	4.17	3.97	"	"
5	Q ₄	1830	7.287	3.96	.72	16866	1022
6	Q ₁	--	5.593	3.70	2.65	"	"
7	Q ₁	1710	7.259	3.87	.77	3985	119
8	Q ₁	--	7.925	3.59	2.73	"	"
9	Q ₁	1715	10.118	3.27	4.38	"	"
10	Q ₀	1718	5.843	3.37	1.05	--	--
11	Q ₀	--	5.496	3.85	3.02	--	--
12	Q ₀	1719	10.146	4.36	4.54	--	--
13	Q ₃	1758	5.357	3.63	2.73	"	"
14	Q ₄	--	6.926	3.27	4.54	"	"
15	Q ₄	--	2.456	3.63	.78	16605	999
16	Q ₂	--	4.982	3.98	4.54	"	"
17	Q ₂	1823	2.984	3.08	2.73	8019	287
18	Q _{4B}	--	4.913	3.33	3.02	"	"
19	Q _{4B}	1815	7.495	3.59	2.84	979	27
20	Q ₁	--	9.299	3.37	5.11	"	"
21	Q ₁	1818	7.134	3.19	.97	3926	118
22	Q ₂	1819	10.229	3.43	4.54	"	"
23	Q ₂	1821	9.410	3.28	.78	7915	279
24	Q _{3A}	--	5.940	3.23	2.77	"	"
25	Q _{3A}	1950	5.288	3.72	.81	1979	57
26	Q ₀	--	5.857	3.72	2.92	"	"
27	Q ₀	--	7.564	3.92	4.54	"	"
28	Q ₀	1955	8.786	3.92	.78	--	--

TABLE A-3 DATA IN FULL-SCALE UNITS (Continued)

BRASH ICE #	Name	Time	R Long Tons	h ft.	v knots	Q _T SCFM	P _T HP
29	↓ Q ₂		8.050	3.78	2.65	--	--
30			7.384	3.33	4.54	--	--
31	↓ Q _{3A}	1554	3.886	3.03	2.73	8050	289
32	↓ Q _{3A}	--	6.801	3.08	4.54	"	"
33	↓ Q ₁	--	6.246	2.89	1.51	1981	57
34	↓ Q ₁	--	7.606	2.98	4.54	"	"
35	↓ Q ₁	--	5.552	3.28	1.51	3968	119
36	↓ Q _{4B}	1611	3.47	3.39	2.77	"	"
37	↓ Q _{4B}	1650	5.829	3.03	1.65	991	28
38	↓ Q _{4B}	--	4.858	3.03	2.65	"	"
39	↓ Q _{4B}	--	5.829	3.13	4.54	"	"
40	↓ Q _{4B}	1700	5.829	3.28	1.44	--	--
41	↓ Q _{4B}	--	4.025	3.00	2.84	--	--
42	↓ Q _{4B}	1703	4.996	3.39	4.54	--	--
43	↓ Q _{3A}	1745	5.135	3.59	2.84	1981	57
44	↓ Q _{4B}	--	4.996	3.19	4.96	"	"
45	↓ Q _{4B}	1748	5.135	3.57	.79	990	28
46	↓ Q _{4B}	--	4.164	3.72	2.89	"	"
47	↓ Q _{4B} *	--	2.22	3.66	3.02	--	--
48	↓ Q _{4B}	1753	4.58	3.52	4.54	--	--

*Deleted from analysis, see Table A-1.

TABLE A-3 DATA IN FULL-SCALE UNITS

STARTING RESISTANCE		Ice Condition	R Long Tons	h ft.	v knots	σ psi.	Q_T SCFM	P_T HP
#	Name							
1	Q ₀	Brash	3.73	2.74	.0398	--	--	--
2	Q ₂	↓	3.67	↓	.0398	8130	292	
3	Q ₄	Solid	6.53	1.69	.0398	16839	1020	
4	Q ₁	↓	20.47	↓	.0398	3993	120	
5	Q ₁	↓	14.08	↓	.0398	3977	119	
6	Q ₀	↓	11.52	↓	.0394	--	--	
7	Q ₀	↓	15.18	1.79	.0391	--	53.80	
8	Q _{4B}	↓	12.89	↓	.0394	1015	29	
9	Q _{3A}	↓	12.96	↓	.0384	1992	57	
10	Q ₁	↓	12.04	↓	.0384	3995	120	
11	Q ₀	↓	18.23	1.71	.0398	--	88.85	
12	Q _{3A}	↓	17.100	↓	.0384	2020	58	
13	Q _{4B}	↓	17.62	↓	.0384	990	28	
14	Q ₁	↓	14.99	↓	.0398	4011	120	
15	Q _{4B}	↓	5.27	3.62	.0356	991	28	
16	Q _{3A}	Brash	7.91	↓	.0371	1981	57	
17	Q ₂	↓	6.57	↓	.0371	8168	294	
18	Q ₀	↓	11.35	↓	.0384	--	--	
19	Q ₀	↓	5.55	↓	.0384	--	--	
20	Q ₀	↓	10.36	↓	.0384	--	--	
21	Q ₀	↓	4.39	↓	.0384	--	--	

APPENDIX B

FRICTION DATA

TABLE B.1 FRICTION AND ROUGHNESS MEASUREMENTS

B-1/B-2

TABLE B.1 FRICTION AND ROUGHNESS MEASUREMENTS

Date	Location	Normal Load, N	Friction Factor, f	Avg. Bottom	Avg. Side	Avg. All	CLA Roughness μm	Avg. Roughness
1-5-77	Port	.98/	.288	.245			1.63	1.27
		2.94/	.191		1.89			
	At Keel	4.09/	.253		1.45			
		.98/	.291		0.98			
		2.94/	.230		0.74			
		4.09/	.249		0.94			
		.98/	.271					
		2.94/	.225					
		4.09/	.207					
		.98/	.278					
2.94/	.278							
4.09/	.207							
1-5-77	Port	.98/	.208	.231			1.19	1.22
		2.94/	.175		1.14			
	At DWL	4.09/	.210		1.32			
		.98/	.245					
		2.94/	.247					
		4.09/	.229					
		.98/	.279					
		2.94/	.286					
		4.90/	.203					
		.98/	.342					
2.94/	.254							
4.90/	.239							
1-6-77	STBD	.98/	.240	.249			1.11	1.15
		2.94/	.188		1.26			
	At DWL	4.90/	.211		1.04			
		.98/	.240		1.43			
		2.94/	.188		0.92			
		4.90/	.211					
		.224	.24		.232			
		.224	.24		.232			
		.224	.24		.232			
		.224	.24		.232			
.224	.24	.232						
.224	.24	.232						

Note: Avg. Sample Size 50 x 50 mm.

APPENDIX C

ICE DATA

TABLE C.1 DAILY ICE PROPERTIES

C-1/C-2

TABLE C.1 DAILY ICE PROPERTIES

SOLID ICE

Date	Avg. Thickness (mm)	Before σ_f kPa	S_{σ_f} kPa	E_E MPa	S_{E_E} MPa	σ_f kPa	E MPa	S_E MPa	Ice Salinity 0/00
1-3-77	19.0	71.26	18.96	15.55	3.41	39.86	5.04	2.15	-
1-4-77	20.7	59.22	10.21	10.67	2.95	28.14	2.61	0.55	3.97
1-5-77	22.7	20.09	6.24	2.46	0.38	16.36	1.57	0.31	-
1-6-77	21.3	32.41	5.70	11.11	1.63	24.12	4.53	0.82	-

Date	Ice Surface Temp °C	Ice Density kg/m ³	Water Salinity 0/00	Water Density kg/m ³	Water Temp. °C
1-3-77	-1.47	.940	4.03	1005	.13
1-4-77	-1.2	.940	4.00	1005	-.43
1-5-77	-	.940	4.00	1005	.13
	-	.940	-	1005	0.1

TABLE C.1 DAILY ICE PROPERTIES (CON'T)

BRASH ICE

Date	Side	Avg. Thickness (mm)	Brash Density (Kg/m ³)	Cone Penetrometer (mm)
1-3-77	-	47.4	-	-
1-4-77	-	46.0	676.4	8
1-5-77	1	42.8	636.4	8.75
	2	47.6	663.1	10.5
1-6-77	1	39.9	692.2	8.42
	2	45.2	508.2	7.17

APPENDIX D

REGRESSION ANALYSIS OF DIMENSIONLESS DATA

TABLE	SOLID ICE	TABLE	BRASH ICE
D.1	Q_0	D.8	Q_0
D.2	Q_{4B}	D.9	Q_{4B}
D.3	Q_{3A}	D.10	Q_{3A}
D.4	Q_1	D.11	Q_1
D.5	Q_2	D.12	Q_2
D.6	Q_3	D.13	Q_3
D.7	Q_4	D.14	Q_4
		D.15	1975 Data, 1.5 Ft. Solid Ice, Q_0 , Model 2

Definition of Variables

	Solid Ice Intercept	Brash Intercept
0		
1	$\frac{R}{\rho_w g B h^2} = R'$	$\frac{R}{\rho_i g B h^2}$
2	$\frac{v}{\sqrt{gh}} = v'$	$\frac{v}{\sqrt{gh}}$
3	$\frac{\sigma}{\rho_w g h} = \sigma'$	$\frac{v^2}{gh}$
4	$v' \times \sigma'$	

The computer printouts contained in this Appendix are the result of forced multiple linear regression to the three pre-selected predictor equation forms.

TABLE D.1

RESISTANCE FOR 00

MULTIPLE LINEAR REGRESSION

NUMBER OF OBSERVATIONS 12
 NUMBER OF VARIABLES 4

INDEX	MEANS	STD DEVS
1	11.3958	3.8444E
2	.628333	.383896
3	181.658	96.1218
4	116.718	106.315

CORRELATION COEFFICIENTS

ROW NUMBER	1	2	3	4	
1		.674056	.638834	.848143	0
2	.674056		.102569	.748696	0
3	.638834	.10257		.644793	0
4	.848143	.748696	.644793		0

SUMS OF SQUARES AND CROSS PRODUCTS

ROW NUMBER	1	2	3	4	
1720.96	96.1833	27436.5	19774.3		0
96.1833	6.28369	1400.44	1209.18		0
27436.5	1400.44	.497631E 06	.326914E 06		0
19774.3	1209.18	.326914E 06	.287608E 06		0

TABLE D.1 (Continued)

REGRESSION NUMBER 1 DEPENDENT VARIABLE 11

1000 0 172.88000 1.44000
 0 0.00000 0.00000
 4 0.00000 0.00000
 STANDARD ERROR OF ESTIMATE= 1.15000
 COEFFICIENT OF VARIATION= 1.18000
 FREQUENCIES 11.00000 11.00000 D.F.= 10

ANALYSIS OF VARIANCE TABLE

	DF	SS	MS	F
REG	1	115.848	115.848	25.5314
RES	10	45.8000	4.58000	

ACTUAL	PREDICTED	RESIDUAL
12.17	11.8700	0.3000
12.84	11.8700	0.9700
12.55	12.0000	0.5500
8.54	11.0000	-2.4600
8.43	11.0000	-2.5700
12.12	12.4000	-0.2800
8.17	8.10000	0.07000
8	8.0000	0.00000
10.41	8.00000	2.41000
8.56	8.40000	0.16000
10.81	8.80000	2.01000
12.55	11.0000	1.55000

DISCRIMINATION COEFF.= .580000

REGRESSION NUMBER 2 DEPENDENT VARIABLE 11

1000 0 172.88000 1.44000
 0 0.13289 1.28173 4.24432
 4 0.75000 0.18812 0.61861
 STANDARD ERROR OF ESTIMATE= 1.0784
 COEFFICIENT OF VARIATION= 1.06139
 FREQUENCIES 11.00000 11.00000 D.F.= 10

ANALYSIS OF VARIANCE TABLE

	DF	SS	MS	F
REG	1	71.0001	71.0001	8.10001
RES	10	62.7000	6.27000	

ACTUAL	PREDICTED	RESIDUAL
12.17	11.8700	0.3000
12.84	11.8700	0.9700
12.55	12.0000	0.5500
8.54	11.0000	-2.4600
8.43	11.0000	-2.5700
12.12	12.4000	-0.2800
8.17	8.10000	0.07000
8	8.00000	0.00000
10.41	11.0000	-0.59000
8.56	8.40000	0.16000
10.81	11.0000	-0.19000
12.55	11.0000	1.55000

DISCRIMINATION COEFF.= .580000 D-3

TABLE D.2

RESISTANCE FOR 04B

MULTIPLE LINEAR REGRESSION



NUMBER OF OBSERVATIONS 5
 NUMBER OF VARIABLES 4

INDEX	MEANS	STD DEVS
1	11.126	1.43713
2	.7176	.381695
3	106.72	21.7913
4	74.2516	41.646

CORRELATION COEFFICIENTS

ROW NUMBER	1				
1		.965659	-.169357	.939286	0
ROW NUMBER	2				
.965659	1		-.355196	.920594	0
ROW NUMBER	3				
-.169357	-.355196	1		.232244E-01	0
ROW NUMBER	4				
.939286	.920594	.232244E-01	1		0

SUMS OF SQUARES AND CROSS PRODUCTS

ROW NUMBER	1				
627.201	42.04	5918.96	4355.48	0	
ROW NUMBER	2				
42.04	3.15812	371.303	324.981	0	
ROW NUMBER	3				
5918.96	371.303	58909.3	39727.2	0	
ROW NUMBER	4				
4355.48	324.981	39727.2	34504.1	0	

TABLE D.2 (Continued)

REGRESSION NUMBER 1 DEPENDENT VARIABLE IS 1

INDEX	B	STD ERROR	T-RATIO
0	8.71928	.567901	15.3535
4	.324130E-01	.683633E-02	4.7413

STANDARD ERROR OF ESTIMATE= .569411

COEFFICIENT OF VARIATION= .511784E-01

R-SQUARED= .98226 R= .99287 D.F.= 3

ANALYSIS OF VARIANCE TABLE				
	DF	SS	MS	F
REG	1	7.28864	7.28864	82.4799
RES	3	.972687	.324229	

ACTUAL	PREDICTED	RESIDUAL
10.21	10.4591	-.249052
12.3	11.428	.871992
9.29	9.42099	-.13099
11.07	11.2333	-.16264
12.76	13.0638	-.323735

DURBIN-WATSON STAT.= 2.35857

REGRESSION NUMBER 2 DEPENDENT VARIABLE IS 1

INDEX	B	STD ERROR	T-RATIO
0	8.51821	.448617	18.9879
2	3.63391	.564477	6.43766

STANDARD ERROR OF ESTIMATE= .431141

COEFFICIENT OF VARIATION= .387509E-01

R-SQUARED= .982499 R= .98566 D.F.= 3

ANALYSIS OF VARIANCE TABLE				
	DF	SS	MS	F
REG	1	7.70368	7.70368	41.4436
RES	3	.557648	.185883	

ACTUAL	PREDICTED	RESIDUAL
10.21	10.8513	-.64128
12.3	12.1849	.115077
9.29	9.15788	.132124
11.07	10.735	.335006
12.76	12.7003	.590620E-01

DURBIN-WATSON STAT.= 1.23875

TABLE D.3

RESISTANCE FOR OSA

MULTIPLE LINEAR REGRESSION

NUMBER OF OBSERVATIONS 5
 NUMBER OF VARIABLES 4

INDEX	MEANS	STD DEVS
1	9.522	3.34983
2	.6018	.430099
3	99.83	41.5031
4	60.4982	57.0118

CORRELATION COEFFICIENTS

ROW NUMBER	1				
1		.687458	.744726	.908406	0
ROW NUMBER	2				
.687458	1		.278681E-01	.839909	0
ROW NUMBER	3				
.744726	.278688E-01	1		.482679	0
ROW NUMBER	4				
.908406	.839909	.482679	1		0

SUMS OF SQUARES AND CROSS PRODUCTS

ROW NUMBER	1				
507.8	32.9145	5220.38	3604.52	0	
ROW NUMBER	2				
32.9145	2.55076	302.534	264.42	0	
ROW NUMBER	3				
5220.38	302.534	56903.4	34792.2	0	
ROW NUMBER	4				
3604.52	264.42	34792.2	31201.5	0	

TABLE D.3 (Continued)

REGRESSION NUMBER 1 DEPENDENT VARIABLE IS 1

INDEX	B	STD ERROR	T-RATIO
0	6.3929	1.12217	5.69692
4	.532752E-01	.141327E-01	3.76339

STANDARD ERROR OF ESTIMATE= 1.61717

COEFFICIENT OF VARIATION= .16907

R-SQUARED= .825207 R= .908409 D.F.= 3

ANALYSIS OF VARIANCE TABLE

	DF	SS	MS	F
REG	1	37.0399	37.0399	14.1632
RES	3	7.84567	2.61522	

ACTUAL	PREDICTED	RESIDUAL
5.63	7.02405	-1.39405
7.93	3.76655	-4.16545
9.86	9.97224	-1.11233
9.95	7.66494	2.28507
14.72	14.6892	.377693E-01

DURBIN-WATSON STAT.= 1.48196

REGRESSION NUMBER 2 DEPENDENT VARIABLE IS 1

INDEX	B	STD ERROR	T-RATIO
0	6.3998	2.33245	2.74391
2	5.35428	3.2556	1.6396

STANDARD ERROR OF ESTIMATE= 2.80907

COEFFICIENT OF VARIATION= .291542

R-SQUARED= .472602 R= .687461 D.F.= 3

ANALYSIS OF VARIANCE TABLE

	DF	SS	MS	F
REG	1	21.213	21.213	2.6863
RES	3	23.6725	7.89085	

ACTUAL	PREDICTED	RESIDUAL
5.63	7.31002	-1.68002
7.95	9.7141	-1.7641
9.86	11.7434	-1.88337
9.95	7.28861	2.66139
14.72	12.0539	2.66608

DURBIN-WATSON STAT.= .873429

TABLE D.4

RESISTANCE FOR Q1

MULTIPLE LINEAR REGRESSION

NUMBER OF OBSERVATIONS 9
 NUMBER OF VARIABLES 4

INDEX	MEANS	STD DEVS
1	10.7679	2.97708
2	.630339	.400427
3	169.389	61.1783
4	108.709	90.312

CORRELATION COEFFICIENTS

ROW NUMBER	1	2	3	4	
1		.913474	.283829	.899645	0
2	.913474		.838891E-01	.856114	0
3	.283829	.838890E-01		.494916	0
4	.899645	.856115	.494916		0

SUMS OF SQUARES AND CROSS PRODUCTS

ROW NUMBER	1	2	3	4	
1114.41	69.3511	16829	12256.1		0
69.3511	4.86492	978.23	837.502		0
16829	978.231	.268176E 06	.185180E 06		0
12256.1	837.502	.185180E 06	.157958E 06		0

TABLE D.4 (Continued)

REGRESSION NUMBER	3	DEPENDENT VARIABLE ID	4
INDEX	5	STD ERROR	T-RATIO
0	11.14137	1.37567	8.0994
4	10.763271	1.311644	8.1973
STANDARD ERROR OF ESTIMATE=		1.3811	
COEFFICIENT OF VARIATION=		.13341	
F-RATIO=		.164714	F= .89944 D.F.=
ANALYSIS OF VARIANCE TABLE			
	DF	SS	MS
REG	1	57.4133	57.4133
RES	7	13.4416	1.92023
TOTAL		PREDICTED	
10.65	11.1111	-1.37107	
10.75	14.507	1.58314	
10.85	8.76365	1.30443	
10.95	11.379	-1.274	
11.05	14.3113	-1.31173	
11.15	7.05443	-1.43712	
11.25	10.0018	1.1751	
11.35	14.1571	-1.11871	
12	10.1437	1.35433	
CORRELATION COEFF.=		.810516	

REGRESSION NUMBER	3	DEPENDENT VARIABLE ID	4
INDEX	5	STD ERROR	T-RATIO
0	6.48213	1.34855	4.77149
4	6.79147	1.14341	5.93957
STANDARD ERROR OF ESTIMATE=		1.325	
COEFFICIENT OF VARIATION=		.19056	
F-RATIO=		.134416	F= .801475 D.F.=
ANALYSIS OF VARIANCE TABLE			
	DF	SS	MS
REG	1	54.164	54.164
RES	7	11.7391	1.67702
TOTAL		PREDICTED	
10.65	11.3254	-1.37543	
10.75	14.7733	1.31145	
10.85	8.55443	1.13317	
10.95	10.9708	-1.21310E-01	
11.05	13.4331	1.15473	
11.15	7.05305	-1.08519E-01	
11.25	10.0018	1.13603	
11.35	14.1574	-1.15114	
12	10.1445	1.35445	
CORRELATION COEFF.=		.811355	

TABLE D.5

RESISTANCE FOR Q2

MULTIPLE LINEAR REGRESSION

NUMBER OF OBSERVATIONS 8
 NUMBER OF VARIABLES 4

INDEX	MEANS	STD DEVS
1	9.74375	5.17008
2	.59775	.418738
3	137.213	36.3665
4	86.0573	73.5642

CORRELATION COEFFICIENTS

ROW NUMBER	1	2	3	4	
1		.937489	.550727	.954196	0
2	.937489		.406921	.965122	0
3	.550727	.406921		.586768	0
4	.954197	.965122	.586768		0

SUMS OF SQUARES AND CROSS PRODUCTS

ROW NUMBER	1	2	3	4	
946.633	60.0222	11420.9	9247.51		0
60.0222	3.99099	688.573	612.665		0
11420.9	688.573	.153886E 06	.105455E 06		0
9247.51	612.665	.105455E 06	97097.7		0

.....TABLE D.5 (Continued).....

REGRESSION NUMBER 1 DEPENDENT VARIABLE IS 1

INDEX	B	STD ERROR	T-RATIO
0	3.97033	.946073	4.19664
4	.670881E-01	.858747E-02	7.81233

STANDARD ERROR OF ESTIMATE= 1.67072

COEFFICIENT OF VARIATION= .171466

R-SQUARED= .910491 R= .954197 D.F.= 6

ANALYSIS OF VARIANCE TABLE				
	DF	SS	MS	F
REG	1	170.36	170.36	61.0325
RES	6	16.7478	2.7913	

ACTUAL	PREDICTED	RESIDUAL
5.63	5.36845	-.232454
17.2	18.0979	-.897949
4.46	5.595	-1.135
8.59	9.79197	-1.20197
4.28	4.82658	-.546576
8.09	7.15152	.938485
14.3	10.8587	3.44133
15.4	15.7599	-.359861

DURBIN-WATSON STAT.= 1.4237

.....REGRESSION NUMBER 2 DEPENDENT VARIABLE IS 1

INDEX	B	STD ERROR	T-RATIO
0	2.94055	1.239	2.37332
2	11.575	1.75419	6.59847

STANDARD ERROR OF ESTIMATE= 1.94343

COEFFICIENT OF VARIATION= .199454

R-SQUARED= .878825 R= .937489 D.F.= 6

ANALYSIS OF VARIANCE TABLE				
	DF	SS	MS	F
REG	1	164.446	164.446	43.5398
RES	6	22.6615	3.77692	

ACTUAL	PREDICTED	RESIDUAL
5.63	4.93145	.698549
17.2	16.3212	.878765
4.46	4.89673	-.436726
8.59	10.2559	-1.66594
4.28	4.7231	-.443101
8.09	9.59617	-1.50617
14.3	10.5222	3.77783
15.4	16.7032	-1.30321

DURBIN-WATSON STAT.= 2.63165 D-11/D-12

TABLE D.6 (Continued)

REGRESSION NUMBER 1 DEPENDENT VARIABLE IS 1

INDEX	B	STD ERROR	T-RATIO
0	4.42394	1.59398	2.81304
4	.502244E-01	.144531E-01	3.475

STANDARD ERROR OF ESTIMATE= 1.29557

COEFFICIENT OF VARIATION= .135732

R-SQUARED= .85791 R= .926235 D.F.= 2

ANALYSIS OF VARIANCE TABLE

	DF	SS	MS	F
REG	1	20.2691	20.2691	12.0756
RES	2	3.35703	1.67851	

ACTUAL	PREDICTED	RESIDUAL
6.39	5.99007	.399932
10.64	10.0736	.566439
8.3	9.88075	-1.58075
12.85	12.2356	.614382

DURBIN-WATSON STAT.= 2.817

REGRESSION NUMBER 2 DEPENDENT VARIABLE IS 1

INDEX	B	STD ERROR	T-RATIO
0	5.11353	1.70998	2.99028
2	6.76333	2.34109	2.88897

STANDARD ERROR OF ESTIMATE= 1.51115

COEFFICIENT OF VARIATION= .158318

R-SQUARED= .806691 R= .89816 D.F.= 2

ANALYSIS OF VARIANCE TABLE

	DF	SS	MS	F
REG	1	19.059	19.059	8.34613
RES	2	4.56714	2.28357	

ACTUAL	PREDICTED	RESIDUAL
6.39	6.27662	.11338
10.64	9.47568	1.16432
8.3	10.0303	-1.73027
12.85	12.3974	.452567

DURBIN-WATSON STAT.= 3.11966

TABLE D.7

RESISTANCE FOR 04

MULTIPLE LINEAR REGRESSION

NUMBER OF OBSERVATIONS 5
 NUMBER OF VARIABLES 4

INDEX	MEANS	STD DEVS
1	10.478	4.94973
2	.6504	.487844
3	230.56	84.2484
4	151.676	125.847

CORRELATION COEFFICIENTS

ROW NUMBER	1	2	3	4	
1		.381073	.483206	.954646	0
2	.381073		.513900E-01	.855049	0
3	.483206	.513900E-01		.464872	0
4	.954646	.85505	.464872		0

SUMS OF SQUARES AND CROSS PRODUCTS

ROW NUMBER	1	2	3	4	
646.942		42.5846	12885	10349.9	0
42.5846	42.5846		758.23	703.229	0
12885	758.23	758.23		.294181E 06	.194567E 06
10349.9	703.23	703.23	.194567E 06		.178378E 06

TABLE D.7 (Continued)

REGRESSION NUMBER 1 DEPENDENT VARIABLE IS 1

INDEX	B	STD ERROR	T-RATIO
0	4.72327	1.13037	4.17853
4	.379409E-01	.598458E-02	6.33978

STANDARD ERROR OF ESTIMATE= 1.50628

COEFFICIENT OF VARIATION= .143756

R-SQUARED= .930544 R= .964647 D.F.= 3

ANALYSIS OF VARIANCE TABLE

	DF	SS	MS	F
REG	1	91.1926	91.1926	40.1928
RES	3	6.80864	2.26955	

ACTUAL	PREDICTED	RESIDUAL
6.77	6.5897	.2003
13.07	11.669	1.40097
16.3	17.5333	-1.23326
4.09	5.54192	-1.45192
12.16	11.0761	1.08391

DURBIN-WATSON STAT.= 2.18301

REGRESSION NUMBER 2 DEPENDENT VARIABLE IS 1

INDEX	B	STD ERROR	T-RATIO
0	4.66377	2.17001	2.1492
2	2.93947	2.77067	3.22647

STANDARD ERROR OF ESTIMATE= 2.70331

COEFFICIENT OF VARIATION= .257998

R-SQUARED= .776288 R= .881072 D.F.= 3

ANALYSIS OF VARIANCE TABLE

	DF	SS	MS	F
REG	1	76.0756	76.0756	10.4101
RES	3	21.9236	7.30786	

ACTUAL	PREDICTED	RESIDUAL
6.77	6.15666	.613342
13.07	10.3761	2.69391
16.3	14.7743	1.52569
4.09	6.12994	-2.03984
12.16	14.9531	-2.7931

DURBIN-WATSON STAT.= .365456

TABLE D.8

REGRESSION FOR NDFPD

MULTIPLE LINEAR REGRESSION

INDEX	MEAN	STD DEV
1	.551	.105573
2	.4712	.237574
3	.27242	.215463

CORRELATION COEFFICIENTS

ROW NUMBER	INDEX	1	2	3
1	1	-1.192226	-1.130245	0
2	2	-1.192226	1	.932939
3	3	-1.130245	.932939	1

SUM OF SQUARED AND CROSS PRODUCTS

ROW NUMBER	INDEX	1	2	3
1	1	2.1307	2.55901	1.49064
2	2	2.55901	2.72487	1.74311
3	3	1.49064	1.74311	1.16543

REGRESSION NUMBER 1 DEPENDENT VARIABLE IS 1

INDEX	B	STD ERROR	T-RATIO
0	.551201	.552861E-01	9.96967
1	-.192226	.165374	-1.17152

STANDARD ERROR OF ESTIMATE = .107152

COEFFICIENT OF VARIATION = .195753

R-SQUARED = .164235E-01 R = .130219 T.F. = 3

ANALYSIS OF VARIANCE TABLE

	DF	SS	MS	F
REG	1	.160517E-02	.160517E-02	.13204
RES	2	.920741E-01	.460370E-01	

ACTUAL	PREDICTED	RESIDUAL
.55	.55142	-.01445E-02
.41	.55497	-.14497
.59	.741274	-.151274E-01
.53	.547035	-.017035E-01
.58	.557768	.022232E-01
.73	.511261	.218739
.59	.544463	.045537E-01
.49	.531196	-.041196E-01
.43	.534529	-.104529E-01
.41	.535554	-.125554

DURBIN-WATSON STAT. = 1.25408 D-17

TABLE D.9

REGRESSION TABLE FOR THE

MULTIPLE CORRELATION

.....

NUMBER OF OBSERVATIONS
 NUMBER OF VARIABLES

INDEX	RAI	ST. DEV.
1	.474333	.184619
2	.477333	.184619
3	.477333	.184619

REGRESSION COEFFICIENTS

REGRESSOR	INDEX	RAI	ST. DEV.	T-RATIO	P
REGRESSOR 1	1	.474333	.184619	2.569	.015
REGRESSOR 2	2	.477333	.184619	2.588	.014
REGRESSOR 3	3	.477333	.184619	2.588	.014
.....					
REGRESSOR 4	4	1.16733	1.16733	1.000	.333
REGRESSOR 5	5	1.16733	1.16733	1.000	.333
REGRESSOR 6	6	1.16733	1.16733	1.000	.333

REGRESSION MODEL DEPENDENT VARIABLE IS

INDEX	R	ST. ERROR	T-RATIO
1	.474333	.184619	2.569
2	.477333	.184619	2.588

STANDARD ERROR OF ESTIMATE = .184619

COEFFICIENT OF VARIATION = .184619

REGRESSOR R ST. ERROR D.F. P

ANALYSIS OF VARIANCE TABLE				
DF	SS	MS	F	P
REG	1	.474333	1.16733	.333
RES	5	.184619	.184619	.333

R	R-SQ	REGRESSOR	REGRESSOR
.474	.224	.474333	.474333
.477	.228	.477333	.477333
.477	.228	.477333	.477333
.477	.228	.477333	.477333
.477	.228	.477333	.477333
.477	.228	.477333	.477333
.477	.228	.477333	.477333
.477	.228	.477333	.477333
.477	.228	.477333	.477333
.477	.228	.477333	.477333

REGRESSION TABLE .184619

TABLE D.10

REGRESSION FOR N0900A

MULTIPLE LINEAR REGRESSION

NUMBER OF OBSERVATIONS 7
 NUMBER OF VARIABLES 3

INDEX	MEAN	STD DEVI
1	.59	.206479
2	.510697	.264197
3	.320843	.264644

CORRELATION COEFFICIENTS

ROW NUMBER	1	2	3
1	1		
2	-.233914E-01	1	
3	-.133912E-01	.920616	1

SUM OF SQUARES AND CROSS PRODUCTS

ROW NUMBER	1	2	3
1	2.3995	2.10208	1.31905
2	2.10208	2.24543	1.55375
3	1.31905	1.55375	1.14081

REGRESSION NUMBER 1 DEPENDENT VARIABLE ID 1

INDEX	B	STD ERROR	T-RATIO
0	.584896	.140823	4.15336
1	-.142540E-01	.146357	-.411457E-01

STANDARD ERROR OF ESTIMATE= .266147

COEFFICIENT OF VARIATION= .293101

R-SQUARED= .241130E-02 R= .156897E-01 D.F.= 5

ANALYSIS OF VARIANCE TABLE

	DF	SS	MS	F
REG	1	.372612E-04	.372612E-04	.170633E-02
RES	5	.259713	.519427E-01	

ACTUAL	PREDICTED	RESIDUAL
.43	.584897	-.154897
.47	.581702	-.111702
.54	.510917	-.070917E-01
.71	.582823	.127177
.72	.583837	.136163
.44	.531748	-.091748
.54	.584339	-.044339E-01

CORRELATION STAT.= 1.49351 D-19

AD-A084 623

ARCTEC INC COLUMBIA MD
MODEL TESTS IN ICE TO CONFIRM EFFECTIVENESS OF THE 140-FOOT WYT--ETC(U)
AUG 77 R A MAJOR DOT-C6-6424A

F/G 13/10

UNCLASSIFIED

354C-2

USCG-E-02-80

NL

2 of 2
AD
AD P 2603



END
DATE
FILMED
6-80
DTIC

TABLE D.11

BRIN PREDICTOR FOR MI

MULTIPLE LINEAR REGRESSION

NUMBER OF OBSERVATION	X	Y
NUMBER OF VARIABLES	1	1
INDEX	MEAN	STD DEVS
1	.682238	.141187
2	.473697	.298089
3	.2659	.233811

CORRELATION COEFFICIENTS

ROW NUMBER	1				
1	.682238	.697939	0	0	
ROW NUMBER	2				
.682238	1	.818474	0	0	
ROW NUMBER	3				
.697939	.818474	1	0	0	

SUMS OF SQUARES AND CROSS PRODUCTS

ROW NUMBER	1				
4.73697	2.14329	1.87343	0	0	
ROW NUMBER	2				
3.14329	2.16812	1.85444	0	0	
ROW NUMBER	3				
1.87343	1.85444	1.69104	0	0	

REGRESSION NUMBER 1 DEPENDENT VARIABLE 10 1

INDEX	B	STD ERROR	T-RATIO
0	.303596	.450257E-01	6.7443
1	.110457	.275539	3.97844

STANDARD ERROR OF ESTIMATION .182181

COEFFICIENT OF VARIATION .265479

F-RATIO .457117 R= .687927 D.F.= 7

ANALYSIS OF VARIANCE TABLE

DF	SS	MS	F
REG 1	.230432	.230432	6.54330
RES 7	.248674	.355249E-01	

ACTUAL	PREDICTED	RESIDUAL
.47	.697939	-.220939
.47	.693128	-.220428
.59	.818474	-.228108
.59	.833124	-.242048
1.74	.87343	.86657
.77	.72048	.04952
.77	.81459	-.04689
.87	.847339	.022661
.71	.84359	-.13359

ADJUSTED R-SQ. = .600172

D-20

TABLE D.12

DATA REGRESSION FOR US

MULTIPLE LINEAR REGRESSION

.....

NUMBER OF OBSERVATIONS: 4
 NUMBER OF VARIABLES: 1

INDEPENDENT VARIABLE: 1
 0 .000000
 1 .411
 2 .181067

STD. ERROR
 0 .000000
 1 .000000
 2 .000000

CORRELATION COEFFICIENTS:

RD NUMBER 1
 1 .0000000000 .0000000000

RD NUMBER 2
 2 .0000000000 .0000000000

RD NUMBER 3
 3 .0000000000 .0000000000

COVARIANCE MATRIX AND INVERSE PRODUCT:

RD NUMBER 1
 1 .0000000000 .0000000000

RD NUMBER 2
 2 .0000000000 .0000000000

RD NUMBER 3
 3 .0000000000 .0000000000

REGRESSION NUMBER 1 DEPENDENT VARIABLE 10

INDEPENDENT VARIABLE 1
 0 .0000000000 .0000000000
 1 .0000000000 .0000000000
 2 .0000000000 .0000000000

CONSTANT ERROR LA ESTIMATE .0000000000

COEFFICIENT OF VARIATION .0000000000

R-SQ .0000000000 F .0000000000

ANALYSIS OF VARIANCE TABLE

	DF	SS	MS	F
REG	1	.0000000000	.0000000000	.000000
RES	4	.0000000000	.0000000000	

INDEPENDENT	REGRESSION	RESIDUAL
.00	.0000000000	.0000000000
.40	.0000000000	.0000000000
.80	.0000000000	.0000000000
.10	.0000000000	.0000000000
.50	.0000000000	.0000000000
.90	.0000000000	.0000000000

DEFINITION STATE .0000000000 D-21

TABLE D.13

BATCH RESISTANCE FOR 13

MULTIPLE LINEAR REGRESSION

.....

NUMBER OF OBSERVATIONS 4
 NUMBER OF VARIABLES 3

INDEX	MEAN	STD DEVI
1	.4425	.116294
2	.4487	.264150
3	.4725	.230459

REGRESSION COEFFICIENTS

REG. NUMBER	1	2	3	4	5
1	.962447	.992503	0	0	0
2	.971243	1	.975722	0	0
3	.962447	.975722	1	0	0

LIST OF SQUARE AND CROSS PRODUCTS

REG. NUMBER	1	2	3	4	5
1	1.0000	1.0000	.546412	0	0
2	1.0000	1.0000	.513911	0	0
3	.546412	.513911	.457002	0	0

REGRESSION NUMBER 1 DEPENDENT VARIABLE Y1 1

INDEX	B	STD ERROR	T-RATIO
1	.87721	.330142E-01	2.65743
2	.751117	.475375E-01	1.571413

STANDARD ERROR OF ESTIMATE= .341557E-01

DIFFERENCE OF VARIATIONS= .904578E-01

ADJUSTED R-SQUARED= .957484 R= .952003 D.F.= 2

ANALYSIS OF VARIANCE TABLE

DF	SS	MS	F
1	.902255E-01	.902255E-01	59.5097
2	.107041E-02	.152411E-02	

UNADJ.	ADJUSTED	RESIDUAL
.23	.233800	-.377500E-02
.42	.424000	-.340074E-01
.45	.413000	.361345E-01
.71	.711111	.118941E-01

LINEAR-TREND STAT.= 2.1413 D-22

TABLE D.14

BRACH RESISTANCE FOR 04

MULTIPLE LINEAR REGRESSION

.....

NUMBER OF OBSERVATIONS 4
 NUMBER OF VARIABLES 3

LINE	MEAN	STD. DEVI.
1	.36	.131145
2	.3325	.270145
3	.1633	.209395

CORRELATION COEFFICIENTS

ROW NUMBER	1	2	3
1	.143899E-01	-.373933E-01	0
2	.143899E-01	.843361	0
3	-.373933E-01	.843361	1

SUM OF SQUARED AND CROSS PRODUCTS

ROW NUMBER	1	2	3	4	5
1	.3625	.5033	.246125	0	0
2	.3625	.652225	.332175	0	0
3	.246125	.332175	.209415	0	0

REGRESSION NUMBER 1 DEPENDENT VARIABLE IS 1

LINE	B	STD. ERROR	T-RATIO
0	.163313	.107135	1.52765
3	-.233642E-01	.44151	-.529185E-01

STANDARD ERROR OF ESTIMATE= .120511

COEFFICIENT OF VARIATION= .462195

R-SQUARED= .140178E-02 R= .374329E-01 D.F.= 3

ANALYSIS OF VARIANCE TABLE

DF	SS	MS	F
REG 1	.133742E-04	.133742E-04	.231533E-02
RES 3	.315107E-01	.105036E-01	

ACTUAL	PREDICTED	RESIDUAL
.31	.133644	.176356
.45	.273345	.176655E-01
.31	.33146	-.17836
.15	.373101	-.221098E-01

CORRELATION COEFF. = .163169

TABLE D.15

REGRESSION FOR 8020

MULTIPLE LINEAR REGRESSION

NUMBER OF OBSERVATIONS: 15
 NUMBER OF VARIABLES: 2

INDEX	MEAN	STD DEVI
1	11.8473	2.29409
2	344.113	105.269

CORRELATION COEFFICIENTS

ROW NUMBER	1	2	3	4
1	.92095	0	0	0
2	.92095	1	0	0

SUM OF SQUARED AND CROSS PRODUCTS

ROW NUMBER	1	2	3	4
2196.13	46568.3	0	0	0
46568.3	.104901E 07	0	0	0

REGRESSION NUMBER 1 DEPENDENT VARIABLE IS 1

INDEX	S	STD ERROR	T-RATIO
1	6.953	.632865	11.137
2	.200699E-01	.235531E-02	3.5211

STANDARD ERROR OF ESTIMATE= .927713

COEFFICIENT OF VARIATION= .781727E-01

R-SQUARED= .942147 R= .920949 D.F.= 13

ANALYSIS OF VARIANCE TABLE

REG	DF	SS	MS	F
REG	1	58.4812	58.4812	72.6091
REG	13	11.1995	.860652	

ACTUAL	PREDICTED	RESIDUAL
11.01	10.2635	.746518
12.98	11.8811	1.07988
6.4	7.56387	-1.10387
13.13	13.4747	-.344666
10.93	11.6684	-.738375
12.32	13.4867	-.666702
11.55	14.7792	-1.22921
11.48	10.7813	.673714
12.47	12.9494	.410556
14.91	13.9333	.97774
9.77	9.12151	.648496
12.89	11.6407	1.24872
12.12	13.1174	-.997421
14.62	14.3639	.256323
9.43	9.44664	-1.01664

COBIN-MATCH STAT.= 1.6297 D-24

APPENDIX E

METHOD OF SCALING BUBBLER SYSTEM CHARACTERISTICS

The laws of similitude governing the modeling of the air bubbler system has been investigated using two different approaches. Each approach begins with the fundamental requirement of ship model testing that forces must be scaled by λ^3 where λ is the geometric scale ratio; that is,

$$\frac{F_{\text{prototype}}}{F_{\text{model}}} = \lambda^3 \quad (\text{E.1})$$

$$\lambda = \frac{L_{\text{prototype}}}{L_{\text{model}}} \quad (\text{E.2})$$

where

F = force

L = length

The first approach was developed by Lewis [7]. He assumes that the geometry of the air plume is similar and that the drag coefficient C_D will be equal in model-scale and full-scale. This leads to the following relationship:

$$\frac{Q_{\text{prototype}}}{Q_{\text{model}}} = \lambda^{5/2} \quad (\text{E.3})$$

where Q = volumetric flow rate of air.

The second approach is based on the work of Kobus [8]. For air discharging through an orifice, he develops the following expression for the buoyant force acting between the orifice and a cross-section at x :

$$F(x) = - \frac{P_{\text{atm}} Q_0}{u_b} \ln \left(1 - \frac{x}{h^*} \right) \quad (\text{E.4})$$

$$h^* = h + \frac{P_{\text{atm}}}{\rho_w g} \quad (\text{E.5})$$

where

\bar{u}_b = mean rising speed of air bubble stream

x = vertical distance above orifice

F = buoyant force

Q_0 = volumetric flow rate of air (STP)

P_{atm} = atmospheric pressure

ρ_w = mass density of water

g = acceleration due to gravity

Kobus [8] also states that the mean rising speed of the bubble is independent of orifice size, spacing, and geometry and is a function of air flow rate only as follows:

$$\bar{u}_b = K(Q_0)^{0.15} \quad (E.6)$$

where K = constant.

The ship modeling laws require that this buoyant force scale according to the following relationship:

$$\frac{[F(x)]_{\text{prototype}}}{[F(x)]_{\text{model}}} = \lambda^3 \quad (E.7)$$

Substituting equation E.6 into equation E.4 and forming the ratio in equation E.7 results in the following:

$$\frac{[(Q_0)^{0.85} \ln(1 - x/h^*)]_{\text{prototype}}}{[(Q_0)^{0.85} \ln(1 - x/h^*)]_{\text{model}}} = \lambda^3 \quad (E.8)$$

Solving for the ratio of air flow rates leads to:

$$\frac{(Q_0)_{\text{prototype}}}{(Q_0)_{\text{model}}} = \lambda^{3.53} \frac{[\ln(1 - x/h^*)]_{\text{prototype}}^{1.18}}{[\ln(1 - x/h^*)]_{\text{model}}^{1.18}} \quad (E.9)$$

Equation E.9 contains x and h , and these cannot be eliminated because P_{atm} cannot be scaled for the model tests.

A comparison of the scaling of the air flow rates by equation E.9 and equation E.3 is made in Table E.1 for the 1/24th scale model of the WYTM. It can be seen that in this case, the scaling using equation E.3 results in higher full-scale air flow rates for a measured model-scale air flow rate.

Since these formulations have not been verified with full-scale air bubbler systems on ships in ice, good engineering judgment dictates that the scaling be done according to the relationship which predicts the higher air flow rates for the full-scale ship. It is, therefore, recommended that equation E.3 be used as the scaling law for air flow; that is:

$$\frac{Q_{\text{prototype}}}{Q_{\text{model}}} = \lambda^{5/2} \quad (\text{E.10})$$

TABLE E.1
RATIO OF AIR FLOW RATES FOR THE 140 FOOT WYTM

	$\frac{(Q_0)_{\text{prototype}}}{(Q_0)_{\text{model}}}$		
<u>x</u> (feet)	Eq. E.8	Eq. E.2	
2	2399*	2822	
6	2280	2822	
12	2086	2822	

$$\begin{aligned}
 h^* &= h + P_{atm} / \rho_w g \\
 &= 12.0 + 33.9 \\
 &= 45.9 \text{ ft.}
 \end{aligned}$$